Compressibility Effects on Ideal and Kinetic Ballooning Modes and Elimination of Finite Larmor Radius Stabilization

M. Kotschenreuther

Institute for Fusion Studies

The University of Texas at Austin

Austin, Texas 78712

Abstract

The dynamics of ideal and kinetic ballooning modes are considered analytically including parallel ion dynamics, but without electron dissipation. For ideal modes and typical tokamak parameters, parallel dynamics predominantly determine the growth rate when β is within ~20–40% of the ideal threshold, resulting in a substantial reduction in growth rate. Compressibility also eliminates the stabilization effects of finite Larmor radius (FLR); FLR effects (when temperature gradients are neglected) can even increase the growth rate above the magnetohydrodynamic (MHD) value. Temperature gradients accentuate this by adding a new source of free energy independent of the MHD drive, in the region of ballooning coordinate corresponding in MHD to the continuum. Analytic dispersion relations are derived demonstrating the effects above; the formalism emphasizes the similarities between the ideal MHD and kinetic cases.

I. Introduction

Present and future toroidal confinement devices operate with β close to the threshold for ideal instability, β_c. Recent theoretical investigations have shown that both kink and ballooning modes have similar thresholds.[1] It is important to understand which modes become unstable first, and then the linear and nonlinear evolution of the resulting instabilities. Kink modes are likely to be catastrophically disruptive, but high mode number ballooning modes are possibly nondisruptive. Most previous analyses of ballooning modes[2,3,4,5,6] have neglected parallel compressional effects. We analytically examine linear ballooning modes when β is not greatly different from β_c here, in both fluid and kinetic regimes, with compressibility. Some numerical results are also given.

The mode dynamics are dominated by sonic compressional effects. In ideal magnetohydrodynamics (MHD), the dynamics of parallel sound wave propagation are crucial to the instabilitiy until β exceeds a second threshold $\beta_c' > \beta_c$. We typically find $\beta_c'/\beta_c \sim 1.2$–$1.4$. The dispersion relation is determined analytically in this region; sonic dynamics predominantly determine the growth rate, rather than Alfvénic dynamics.

In Ideal MHD, compressional dynamics lead to a reduction of the growth rate by factors of typically ~4 when compared with growth rates obtained by reduced MHD models neglecting sonic physics. The expansion energy is absorbed by resonant production of parallel kinetic energy and fluid compression. In lower collisionality regimes, the growth rates are shown to be further reduced by resonant ion Landau damping.

Given the small MHD growth rate with compressibility, finite Larmor radius (FLR) effects become more important. In particular, the total diamagnetic frequency ω_* can be of order the MHD growth rate γ_{MHD} for quite low mode numbers when $\beta \sim \beta_c'$ (n~5) for PDX or Doublet III); simple models[3,4] which neglect compressibility, find stability when $\omega_* > 2\gamma_{MHD}$.

However, we find here that compressibility effects nullify FLR stabilization. First, we consider the case where only density gradients are present in the equilibrium. For $\beta \lesssim \beta_c'$, the growth rates are not substantially reduced from the MHD values, even though previous models[3,4] would predict stability. Often, the growth rates are actually increased. We believe this could be interpreted as the destabilization of a positive energy wave by negative dissipation. In the fluid case, the dissipation is the resonant emission of sound waves propagating along field lines; in the kinetic case, it is Landau damping. The coupling to parallel dynamics and perpendicular compression is strong in the ideal MHD case for $\beta \lesssim \beta_c'$; thus the dissipation is strong, totally nullifying any stabilizing FLR influence.

Seyler and Freidberg[7] have found that collisionless ion resonances eliminate absolute FLR stabilization in a screw pinch, without temperature gradients, but the ''residual'' instabilities had small growth rate. Here, we clarify the connection between resonant ion effects and MHD fluid compressibility, and see that the ''residual'' instabilities can have growth rates comparable to MHD for tokamaks.

When ion temperature gradients are included, a new source of driving energy is introduced for collisionless ions. In an MHD ballooning mode, the pressure drive occurs at small ϑ. With temperature gradients, energy is introduced in the large ϑ region corresponding to the ballooning continuum of MHD. Because of this, at $\beta = \beta_c$ the instabilities have a growth rate which is equivalent to that arising in the pure MHD case when β exceeds β_c by 20-30%. This can also lead in principle to an instability independent of the MHD drive. An initial wave packet would propagate in ϑ space till it reaches large enough ϑ for dissipative effects (ignored here) to produce damping (such as drift resonance dissipation). Whether or not there is an unstable eigenmode for $\beta < \beta_c$ depends on the distance in ϑ at which dissipation becomes important. This distance is not extremely long for realistic aspect ratio. The analysis to including dissipation is rather complicated with parallel dynamics; only a few general features are qualitatively discussed.

Generally when FLR is included, the growth rates are always largest when $\omega_* \sim \varepsilon^{1/2}\omega_A \sim \omega_s$, where ω_A and ω_s are the toroidal transit frequencies of Alfvén and sound waves. This is true both with and without temperature gradients. We thus expect that mode numbers corresponding to $\omega_* \sim \varepsilon^{1/2}\omega_A$ are the first to become unstable as β approaches β_c.

The stability analysis of kinetic ballooning modes without parallel dynamics has been considered purely numerically by Hastie and Hasketh[5] and Cheng.[6] We will see here, however, the strongest instabilities occur in the parameter range where the frequency is of the order of the ion thermal transit frequency; thus, parallel dynamics cannot be neglected. More recently, Teng[8] et al., have performed very complete numerical computations for these modes. The results here are analytical. However, we have not quantitatively treated the full eigenmode calculation when dissipation at large ϑ is important; this is treated by the authors above. Simultaneously with the present work, Dominguez and Moore[9] have examined temperature gradient driven instabilities both numerically and analytically, but neglecting parallel dynamics.

The analysis of the ideal MHD case reveals important subtleties in the mode dynamcis for $\beta_c < \beta < \beta_c'$. Important features of the pressure dynamics are well extended along the field lines, i.e., at large values of the ballooning angle coordinate ϑ. These dynamics determine the growth rate, so it is not appropriate to think of the mode as having a typical parallel wavelength of the connection length.

The importance of the extended structure in ϑ space can be understood heuristically using the standard variational prinicple of ideal MHD for the growth rate. We will see that trial functions which have a naive behavior (e.g., are incompressible) at large ballooning angle can give a growth rate which is only infinitesimally positive.

The quantitative analysis begins by reformulating the variational principle to eliminate the difficulties at large ϑ. The growth rate is computed using a trial function which is equal to the eigenfunction for marginal stability of small ϑ, and is found from a two space scale analysis at large ϑ. We show in an Appendix that then the variational formulation is equivalent to asymptotic matching; however it is more computationally convenient. The variational principle can be generalized to the kinetic case, and also to include FLR effects (at the expense of becoming complex rather than real). Analytic techniques similar to those used here in the MHD case can then be used for the kinetic analysis.

Though we restrict our attention here to linear theory, we believe that the insight gained from this work will be needed in constructing proper nonlinear theories of those modes in the present β regime. In particular, the modifications of the linear dynamics by nonlinear effects is quite different for Alfveńic processes and parallel ion sonic processes. The latter dominate the linear analysis, but they have been omitted in common nonlinear models.[10] Also, the importance of the pressure response at large ϑ may indicate a particular sensitivity to nonlinear effects, which are often most important there.

In Sec. II we give simple arguments for the importance of compressibility. These precisely define β_c', and explain why important features of the mode are well extended along the field lines. Motivated by these considerations, in Sec. III we obtain a variational principle for ideal MHD case, and then the dispersion relation. In Sec. IV numerical results are presented to check the range validity of this result for $\beta \gtrsim \beta_c'$. In Sec. V a kinetic formulation of this problem is given using the ballooning equations of Antonsen and Lane.[11] Then the dispersion relation is derived for collisionless ions, but neglecting FLR effects. In Sec. IV FLR effects are examined in both fluid and collisionless ion regimes.

II. Simple Arguments for the Importance of Compressibility

MHD stability is examined using the energy principle, $\Delta W(\underset{\sim}{\xi})$, for the energy released from a given plasma displacement $\underset{\sim}{\xi}$. The maximum growth rate can be found from the variational expression

$$\gamma^2 = -\Delta W(\underset{\sim}{\xi})/I(\underset{\sim}{\xi}) \tag{1}$$

where $I = \int dx\rho|\xi|^2$ is the inertia. These simplify for the case of high mode number ballooning modes,[12] which we consider here. We use flux coordinates $\underset{\sim}{B} = \underset{\sim}{\nabla}\psi \times \underset{\sim}{\nabla}(q\vartheta-\zeta)$, and $J = [\nabla\psi(\nabla\vartheta\times\nabla\zeta)]^{-1}$. Then

$$\Delta W_B = \frac{1}{\bar{J}}\int_{-\infty}^{+\infty} d\vartheta J\left[\frac{|\nabla S|^2}{JB^2}\left(\frac{\partial\chi}{\partial\vartheta}\right)^2 - 2\kappa_\omega\frac{\partial p}{\partial\psi}\chi^2 + \frac{B^2\Gamma p}{B^2+\Gamma p}\left(\frac{1}{J}\frac{\partial\xi_\parallel}{\partial\vartheta} - 2\kappa_\omega\chi\right)^2\right] \tag{2}$$

$$I_B = \frac{1}{\bar{J}}\int_{-\infty}^{+\infty} d\vartheta J\rho\left(\frac{|\nabla S|^2}{B^2}\chi^2 + B^2\xi_\parallel^2\right) . \tag{3}$$

We consider systems with shear, so that ϑ ranges from $-\infty$ to $+\infty$. The quantity χ is the stream function for $\xi_\perp$, $\kappa_\omega = (\hat{b}\cdot\nabla\hat{b}) \times B\cdot\nabla S/B^2$, $\hat{b} = \underset{\sim}{B}/|B|$, $p(\psi)$ and $\rho(\psi)$ and the equilibrium pressure and density, ∇S is the gradient of the eikonal, and $\oint d\vartheta J = \oint d\ell/B$. We take $\nabla S = \nabla(q\vartheta-\zeta)$, valid for axisymmetry. $\bar{J}$ is a convenient normalizing factor with units of J, and Γ is the ratio of specific heats.

The first term in ΔW_B is line bending, the second is pressure drive and the third is from compression, $(\nabla\cdot\xi_\parallel+\nabla\cdot\xi_\perp)^2$. $\nabla\xi_\parallel \propto \partial\xi_\parallel/\partial\vartheta$, and $\nabla\cdot\xi_\perp \propto \kappa_\omega\chi$. The kink term has been neglected and is small as the mode number $\rightarrow \infty$.

The dynamical equations are

$$\frac{1}{J}\frac{\partial}{\partial\vartheta}\frac{|\nabla S|^2}{JB^2}\frac{\partial\chi}{\partial\vartheta} + 2\kappa_\omega\left[p'(\psi)\chi - \frac{B^2\Gamma p}{B^2+\Gamma p}\left(\frac{1}{J}\frac{\partial\xi_\parallel}{\partial\vartheta} - 2\kappa_\omega\chi\right)\right] = \gamma^2\frac{\rho}{B^2}|\nabla S|^2\chi \qquad (4)$$

and

$$\frac{1}{J}\frac{\partial}{\partial\vartheta}\left(\frac{B^2\Gamma p}{B^2+\Gamma p}\right)\left(\frac{1}{J}\frac{\partial\xi_\parallel}{\partial\vartheta} - 2\kappa_\omega\chi\right) - \gamma^2\rho B^2\xi_\parallel = 0 \ . \qquad (5)$$

Computations of the critical β for instability, β_c, proceed by taking $\nabla\cdot\xi = 0$, and then minimizing ΔW. The Euler equation for the minimization χ at marginal stability, χ_c, solves Eq. (5) with $\gamma=0$ and $\nabla\cdot\xi_\parallel = -\nabla\xi_\perp$.

Physically, the dynamics associated with parallel sound wave propagation determine $\xi_\parallel$. These dynamics are important insofar as the cancellation between $\nabla\cdot\xi_\parallel$ and $\nabla\cdot\xi_\perp$ is important. If $\nabla\cdot\xi_\parallel$ is neglected entirely, then a higher β is needed to make $\Delta W < 0$, since $(\nabla\cdot\xi_\perp)^2$ is always stabilizing. Define β_c' to be the β for which $\Delta W > 0$ when $\xi_\parallel$ is neglected. If β_c' is substantially larger than β_c, then the parallel dynamics are important.

For realistic aspect ratio ε (ε=.07) numerical calculations of β_c' exceed β_c by 20%–40%, using the model of Connor et al.[13] for the geometrical coefficients (see Sec. IV). (Note that the relevant ε is the ratio of pressure gradient scale to major radius; the former can be small due to pressure profile peaking.) Figure 1 shows β_c and β_c' versus the shear parameter $\hat{s}$. Since the perpendicular compressibility term is formally of order ε, one might expect $\beta_c'-\beta_c \sim \varepsilon$. In fact, $\beta_c'-\beta_c \sim \varepsilon^\nu$, and here $\nu = 1/2$. Fractional powers of realistic ε are not particularly small. Thus we expect that β_c' can significantly exceed

β_c. It is instructive to examine the matrix element which arises in first order perturbation theory to give the increase in β_c when $|\nabla\cdot\xi_\perp|^2$ is included,

$$\int_{-\infty}^{+\infty} d\vartheta J \frac{B^2\Gamma p}{B^2+\Gamma p} (2\kappa_\omega)^2\chi_c^2 . \tag{6}$$

As $\vartheta\to\infty$, $\kappa_\omega^2 \to \vartheta^2$. The asymptotic behavior of χ_c depends on the Mercier parameter D_I; $D_I > 1/4$ for localized interchange instability. At large ϑ, $\chi_c \to \vartheta^{-1/2-\nu}$, where

$$\nu = \sqrt{1/4-D_I} . \tag{7}$$

Thus $\kappa_\omega^2\chi_c^2 \to \vartheta^{1-2\nu}$, and for $D_I > -3/4$, the matrix element is infinite. Therefore, $\beta_c'-\beta_c$ is not linearly proportional to ε, but some fractional power of ε.

Thus, the parallel dynamics are particularly important in the shaded parameter region in Fig. 1, since without $\nabla\cdot\xi_\parallel$ to cancel $\nabla\cdot\xi_\perp$ there is no instability, i.e., $\Delta W > 0$. The importance of $\nabla\cdot\xi_\parallel$ leads to sharp reduction of the growth rate in this region.

The dynamical equations imply that $\nabla\cdot\xi_\parallel + \nabla\cdot\xi_\perp << \nabla\cdot\xi_\perp$ only if the mode frequency is less than the transit frequency of sound waves, $\omega_s = v_s/qR$. Therefore, in the shaded region of Fig. 1, the growth rate must be less than ω_s. ω_s is typically much less than the Alfvén frequency. Therefore, the actual growth rate past marginal stability is much smaller than might be naively expected.

The dynamics of ballooning modes are surprisingly subtle in the regime between β_c and β_c'. Two inter-related features are 1) important facets of the pressure dynamics extend out to large ϑ (even though the expansion energy input is at $\vartheta \sim 1$) 2) substantial energy is absorbed by resonant sonic effects, i.e., at $\vartheta \sim \omega_s/\gamma$, where $\omega_s \sim v_s/qR_0$, v_s is the sound speed and R_0 the major radius. Feature 1) implies that effects which operate most strongly at large ϑ, (such as turbulent diffusion or certain FLR effects) could disproportionately affect the mode. Feature 2) leads to the nullification of FLR stabilization even in a purely fluid compressible theory.

To illustrate the failure of a naive incompressible picture to describe the dynamics, it is instructive to attempt to estimate the growth rate of the ballooning mode using Eqs. (1)–(3) with an incompressible trial function. Such trial functions give a growth rate which is only infinitesimally positive.

This is surprising, since such trial functions would seem eminently suitable. Consider the following simple procedure to find γ^2 near marginal stability, which is equivalent to standard perturbation theory. Near β_c, the true solution χ of Eqs. (2)–(3) apparently differs from χ_c by an amount proportional to $\beta/\beta_c - 1$. Thus $\Delta W \sim \beta/\beta_c - 1$. We also expect from Eq. (5) that near marginal stability $\partial\xi_{\parallel}/\partial\vartheta = 2J\kappa_\omega\chi_c + O(\beta/\beta_c - 1) + O(\gamma^2)$. Owing to the variational property of Eq. (1), for small $\beta/\beta_c - 1$ (and thus small γ^2), we could use χ_c and $\xi_{\parallel} = \int d\vartheta 2J\kappa_\omega\chi_c$ to compute γ^2 to <u>second</u> <u>order</u> accuracy in $(\beta/\beta_c - 1)$. This gives $\gamma^2 \sim \beta/\beta_c - 1$, with errors $\sim (\beta/\beta_c - 1)^2$.

This perturbation procedure to give the growth rate fails when $D_I > -3/4$. Using the marginal stability equation for χ_c, we have

$$\xi_{\|}(\vartheta) = 2 \int_{-\infty}^{\vartheta} J\kappa_{\omega}\chi_c = \frac{|\nabla S|^2}{JB^2} \frac{\partial \chi_c}{\partial \vartheta} . \tag{8}$$

As $\vartheta \to \infty$, $|\nabla S|^2 \to \vartheta^2$. Thus $\xi_{\|}^2 \sim \vartheta^{1-2\nu}$. For $D_I > -3/4$, the $\xi_{\|}^2$ term in I_B is thus infinite and the estimated growth rate $\Delta W/I$ is only infinitesimally positive.

An accurate analysis of the dynamics to obtain γ^2 must include coupling to sound waves with finite γ in Eq. (5). The need to include γ^2 to resolve a singularity in the propagator of Eq. (5) identifies this as a resonant effect.

More specifically, the growth rate is not determined by balancing the expansion energy against the Alfvén inertia. Rather, when not too far from marginal stability, the expansion energy is absorbed by compression and the resonant production of sonic kinetic energy, for realistic aspect ratio and shear.

Insight into the relative importance of Alfvénic and sonic physics is important, since modifications of the linear ideal MHD due to kinetic or nonlinear ideal effects are very different for the Alfvénic physics and the sonic physics.

Also note that the Alfvénic inertia term in Eq. (3) is infinite as well, since $\vartheta^2\chi_c^2 \sim \vartheta^{1-2\nu}$. Thus an analytic comparison of the relative importance of Alfvénic and compressible effects is nontrivial.

For ballooning modes, the dynamics have often[3,4,10] been approximated in MHD calculations in a way which is equivalent to setting

$$\gamma^2 I_\perp = \gamma^2 \frac{1}{J} \int d\vartheta J \, \rho \frac{|\nabla S|^2}{B^2} \chi^2$$

$$= \frac{1}{J} \int_{-\infty}^{+\infty} d\vartheta \; J \left[\frac{|\nabla S|^2}{JB^2}\left(\frac{\partial \chi}{\partial \vartheta}\right)^2 - 2\chi_\omega \rho' \chi^2\right] , \tag{9}$$

where $\gamma^2 I_\perp$ is the kinetic energy from perpendicular motion. This neglects all compressibility effects,

$$k(\xi) = \int dx \; \gamma^2 \xi_\parallel^2 + (\nabla \cdot \xi)^2 \; . \tag{10}$$

We will see that for ballooning modes with realistic aspect ratio, $k(\xi)$ is significantly larger than $\gamma^2 I_\perp$, for β significantly past marginal stability. For finite shear and realistic ε, this defect is <u>not</u> remedied by augmenting $I_\perp$ by a factor of $1+2q^2$, as was found for small shear.[14] A substantial part of $k(\xi_\parallel)$ arise from the near resonance in the sound wave propagator when $\gamma^2 < \omega_s^2$.

We now derive a dispersion relation near marginal stability which demonstrates the quantitative importance of this resonance. This dispersion relation is approximately valid when $\varepsilon \sim \beta$ is small. Numerical computations using the model curvature show that this relation is reasonably accurate even for $\beta \sim \beta'_c$.

III. Dispersion Relation Near Marginal Stability

We now obtain an alternative variational principle to find γ for β near β_c. This principle does not suffer from the defects of the previous attempt as regards compressibility. It also clarifies the importance of resonant compressibility effects. It will be possible to write the kinetic ballooning equations in a similar variational form in Sec. V, allowing analysis using similar techniques.

The dispersion relation requires a single numerical parameter whose exact evaluation requires that χ_c be known. We will use χ_c as the trial function for small ϑ. At large ϑ, the trial function must include the Alfvén modifications of χ_c, which are obtained using a two-scale analysis. For simplicity, a simple trial function is used in the exterior region which is rigorously valid with a subsidiary aspect ratio expansion. The variational procedure used here is shown to be equivalent to an asymptotic matching procedure in Appendix A.

A. Variational Form

We assume for simplicity that the coefficients in Eqs. (2)-(3) are symmetric in ϑ, and look for a symmetric solution. This is the usual case since most tokamaks have up-down symmetry.

First, we define

$$f = \frac{B^2 \Gamma p}{(B^2 + \Gamma p)} \left[\frac{1}{J} \frac{\partial \xi_{\parallel}}{\partial \vartheta} - 2 \kappa_{\omega} \chi\right] \tag{11}$$

f satisfies

$$\frac{\partial}{\partial\vartheta}\frac{1}{JB^2}\frac{\partial}{\partial\vartheta}f-\rho\gamma^2 J\left(\frac{B^2+\Gamma p}{B^2\Gamma p}\right)f=\gamma^2\ \rho 2J\kappa_\omega\chi\ . \tag{12}$$

We henceforth choose coordinates so that JB^2 is independent of ϑ; this simplifies the inversion of Eq. (12). Define $\bar{J}=\frac{1}{2\pi}\int d\vartheta J$, and define the average < > by

$$\langle A\rangle=\frac{1}{2\pi}\oint d\vartheta JA/\bar{J}\ .$$

Define the ion sound transit frequency by

$$\omega_s^{-2}=\rho\bar{J}^2\left\langle\frac{B^2+\Gamma p}{B^2\Gamma p}\right\rangle\langle B^2\rangle\simeq\frac{\rho q^2R^2}{\Gamma p}\ . \tag{13}$$

where R is the major radius; the approximation is valid for small ε. Note that for components of f which slowly with ϑ, f satisfies

$$\left(\frac{\partial^2 f}{\partial\vartheta^2}-\frac{\gamma^2}{\omega_s^2}f\right)=\frac{\gamma^2}{\omega_s^2}\frac{\Gamma\bar{p}}{\bar{J}}\,2J\kappa_\omega\chi\ . \tag{14}$$

where $\bar{p}=p(\psi)/\langle 1+\Gamma p/B^2\rangle$.

It is useful to note the size of the various terms in Eqs. (2)-(3) for $\beta\sim\varepsilon$. We have $\nabla\cdot\xi\sim 1/R\sim J\sim 1/\varepsilon$, $B\sim\psi\sim\nabla S\sim\rho\sim 1$, and $\kappa\sim r\sim p'\sim\varepsilon$. Also $\omega_s^2/\omega_A^2\sim\beta$ and for $\gamma/\omega_s\sim 1$, $f/\chi\sim\varepsilon^2$.

The variational form is found by inverting Eq. (12) using a Green's function $H(\vartheta,\vartheta')$

$$f = \frac{2\Gamma\bar{p}}{\bar{J}} \frac{\gamma^2}{\omega_s^2} \int_{-\infty}^{+\infty} d\vartheta' \ H(\vartheta,\vartheta') J(\vartheta') \kappa_\omega(\vartheta') \chi(\vartheta') \ . \tag{15}$$

Then we have

$$V = -\gamma^2 \frac{1}{\bar{J}} \int d\vartheta J \frac{p}{B^2} |\nabla S|^2 \chi^2 + k(f)$$

$$\frac{1}{\bar{J}} \int d\vartheta J \left[- \frac{|\nabla S|^2}{J^2 B^2} \left(\frac{\partial \chi}{\partial \vartheta}\right)^2 + 2p' \kappa_\omega \chi^2 \right] \tag{16}$$

where $k(f) = \int d\vartheta J \kappa_\omega \chi f$

$$= \frac{4\Gamma\bar{p}}{\bar{J}^2} \frac{\gamma^2}{\omega_s^2} \int d\vartheta \int d\vartheta' \ J(\vartheta) \kappa_\omega(\vartheta) \chi(\vartheta) H(\vartheta,\vartheta') J(\vartheta') \kappa_\omega(\vartheta') \chi(\vartheta') \ . \tag{17}$$

Note that $k(f)$ is the same as Eq. (10), and it gives the energy absorbed by sonic kinetic energy and compression. Taking $\delta V = 0$ gives the equation for χ, so V is accurate to second order in perturbations to χ.

It may not be immediately apparent that this is an improvement over Eqs. (1)-(3); nonetheless V allows us to obtain an analytic dispersion relation.

Define the Fourier transform of the term driving compression in Eq. (12),

$$\Phi(k) = \int_{-\infty}^{+\infty} d\vartheta \ e^{-ik\vartheta} J(\vartheta) \kappa_\omega(\vartheta) \chi(\vartheta) \ . \tag{18}$$

As will be argued shortly, for $\gamma^2/\omega_s << 1$,

$$k(f) = \frac{-4\Gamma\bar{p}}{\bar{J}^2} \frac{\gamma^2}{\omega_s^2} \int_{-\infty}^{+\infty} \frac{dk}{2\pi} \frac{|\Phi(k)|^2}{k^2+\gamma^2/\omega_s^2} . \tag{19}$$

Here χ is real, so $|\Phi(k)|^2$ appears in the numerator. The denominator of the integrand is the fluid propagator. The problem of an infinite sonic contribution in Sec. II arose from taking $\gamma=0$ in the propagator. k(f) is clearly negative definite, and its magnitude monotonically increases with γ.

Resonant contributions of k(f) arise from the region $\gamma^2/\omega_s^2 \sim k^2$. Nonresonant contributions arise from $k^2 \sim 1$, most of which come from $\vartheta \sim \omega_A/\omega$.

Note that most of the contribution to $\Phi(k)$ for $k \sim \gamma/\omega_s \lesssim 1$ arises from the region $\vartheta\sim1$ (at least for $D_I \leqslant 0$). A crucial ingredient of the analytic dispersion relation is that it is possible to compute the small k behavior of $\Phi(k)$ for $\chi = \chi_c$, without knowing the detailed structure of χ_c, by using the fact that χ_c satisfies the Euler differential equation for ΔW.

B. Trial Function

For $\vartheta\sim1$, and small β/β_c-1 and γ^2, χ can be found by perturbing around χ_c,

$$\frac{\partial}{\partial\vartheta} \left(\frac{|\nabla S|^2}{JB^2}\right)_c \frac{\partial}{\partial\vartheta} \delta\chi + 2(p'J\kappa_\omega)_c\delta\chi = 2\delta(p'J\kappa_\omega)\chi_c$$

$$- \frac{\partial}{\partial\vartheta} \delta\left(\frac{|\nabla S|^2}{JB^2}\right) \frac{\partial}{\partial\vartheta} \chi_c - 2(p'J\kappa_\omega)_c f + \gamma^2 \left(\frac{J\rho|\nabla S|^2}{B^2}\right)_c \chi_c \tag{20}$$

where the subscript c denotes that the quantity is to be evaluated at $\beta = \beta_c$, and δ denotes the perturbation away from the value at $\beta = \beta_c$.

At lowest order for f we have f = constant. If we were to proceed with this technique, the asymptotic behavior would be matched to the solution for $\vartheta >> 1$. Use of the variational principle elminates the need to solve for $\delta\chi$ explicitly. It is sufficient here to note that χ_c is a suitable trial function in this region, since $\delta\chi \sim \beta/\beta_c - 1$.

We now solve Eqs. (2), (12) for $\vartheta >> 1$. This problem was considered neglecting compressibility by Van Dam,[15] who notes that two space scale analysis is possible when $\gamma/\omega_A << 1$. We have $\chi = \bar{\chi} + \tilde{\chi}$, where $\bar{\chi}$ varies slowly with ϑ, and $\tilde{\chi}$ on the scale ~1. Also $\bar{\chi} >> \tilde{\chi}$, but $\partial\bar{\chi}/\partial\vartheta \sim \partial\tilde{\chi}/\partial\vartheta$. At large ϑ, $\kappa \to \vartheta(q'/2p'J)\partial\sigma/\partial\vartheta$ where $\sigma = \nabla\times B \cdot B/B^2$, and $|\nabla S| \to q'|\nabla\psi|\vartheta$.

For components of f which vary slowly in ϑ, the left side of Eq. (12) is

$$\left(\frac{1}{JB^2}\right)\left(\frac{\partial^2}{\partial\vartheta^2} - \frac{\gamma^2}{\bar{\omega}_s^2}\right)\bar{f} \ .$$

This is also a good approximation to the operator for $\tilde{f}$, since the second term is small for $\gamma^2/\omega_s^2 << 1$ in any case. We thus have Eq. (14) for $\bar{f}+\tilde{f}$ when $\gamma^2/\omega_s^2 << 1$.

After manipulations similar to those in Ref. 15 (some of the details of which are given in Appendix B), we obtain

$$\frac{\partial}{\partial\vartheta}\vartheta^2\frac{\partial}{\partial\vartheta}\bar{\chi} + \frac{H}{p'}\frac{\partial}{\partial\vartheta}\vartheta\bar{f} + (\bar{\chi} + \frac{\bar{f}}{p'})D_I = \gamma^2\rho\bar{J}^2\langle B^2/|\nabla\psi|^2\rangle\langle\frac{|\nabla\psi|^2}{B^2}\rangle M\bar{\chi} \tag{21}$$

$$\frac{\partial^2\bar{f}}{\partial\vartheta^2} + \frac{\gamma^2}{\bar{\omega}_s^2}\bar{f} = \frac{\gamma^2}{\bar{\omega}_s^2}\frac{\Gamma\bar{p}q'^2}{\bar{J}^2\langle B^2/|\nabla\psi|^2\rangle}[(E+F)(\bar{\chi}+\bar{f}/\bar{p}) - H\vartheta\frac{\partial\bar{\chi}}{\partial\vartheta}] \tag{22}$$

with $$M = \langle\frac{|\nabla\psi|^2}{B^2}\rangle^{-1}[\langle\frac{|\nabla\psi|^2}{B^2}\rangle + \frac{1}{p'^2}(\langle\sigma^2B^2\rangle - \frac{\langle\sigma B^2\rangle^2}{\langle B^2\rangle})] \tag{23}$$

where $\langle A\rangle_M = \int\frac{d\vartheta}{2\pi}A$

$$E = (p'/q'^2)\langle JB^2/|\nabla\psi|^2\rangle_M\langle 2J[\hat{\underset{\sim}{b}}\cdot\underset{\sim}{\nabla}\hat{\underset{\sim}{b}}\times\underset{\sim}{B}\cdot(q\underset{\sim}{\nabla}\vartheta-\underset{\sim}{\nabla}s)]/B^2\rangle_M \tag{24}$$

$$F = (1/q'^2)\langle JB^2/|\nabla\psi|^2\rangle_M(\langle J\sigma^2B^2/|\nabla\psi|^2\rangle_M - \langle J\sigma B^2/\nabla\psi^2\rangle_M^2/\langle JB^2/|\nabla\psi|^2\rangle_M) \tag{25}$$

$$H = (1/q')\langle JB^2/|\nabla\psi|^2\rangle_M(\frac{\langle J\sigma B^2/\nabla\psi^2\rangle_M}{\langle JB^2/|\nabla\psi|^2\rangle_M} - \langle J\sigma B^2\rangle_M/\langle JB^2\rangle_M) \tag{26}$$

are standard geometrical quantities[16] and $D_I = E+F+H$.

We solve these equations when the coupling between $\bar{\chi}$ and $\bar{f}$ is weak in the large ϑ region. Note the $\bar{f}$ still affects the solution in the inner region, Eq. (20). The coupling is weak when <u>either</u> 1) $\beta\sim\varepsilon$ is small. Then $E \sim F \sim H \sim 1$. However $\bar{f}/p' \sim \varepsilon$ relative to $\bar{\chi}$, so $\bar{\chi}$ can be solved independently of $\bar{f}$ in lowest order; 2) E+F and H are both small. Note that when E+F = 0 and H=0, <u>all</u> of the generic difficulties with singularities noted in Sec. II <u>still</u> apply with full force, since they arise when $-3/4 < E+F+H < 1/4$.

Thus the Alfvén solution $\bar{\chi}_A$ for weak coupling is

$$[(\frac{\partial}{\partial\vartheta}\vartheta^2\frac{\partial}{\partial\vartheta}\bar{\chi}_A) + D_I\bar{\chi}_A] = \frac{\gamma^2}{\omega_A^2}\vartheta^2 M\bar{\chi}_A \ . \tag{27}$$

where we have defined the toroidal Alfven transit frequency by

$$\frac{1}{\omega_A^2} = \rho\langle\frac{B^2}{|\nabla\psi|^2}\rangle\langle\frac{|\nabla\psi|^2}{B^2}\rangle\bar{J}^2 \ . \tag{28}$$

The solution to Eq. (25) is found using modified Bessel's functions,

$$\bar{\chi}_A = \chi_\infty\lambda^{-\nu}2^{1-\nu}\,\vartheta^{-1/2}K_\nu(\lambda\vartheta)/\Gamma(\nu) \tag{29}$$

where $$\lambda^2 = \gamma^2 M/\omega_A^2 \ . \tag{30}$$

For small ϑ,

$$\chi \to \chi_\infty\vartheta^{-1/2-\nu}[1 + \frac{\lambda^2\vartheta^2}{4(1-\nu)}] - \chi_\infty\frac{(1/2)^{2\nu}\Gamma(-\nu)\lambda^{2\nu}\vartheta^{-1/2+\nu}}{\Gamma(\nu+1)} \ . \tag{31}$$

Note that when $\gamma^2/\omega_A^2 << 1$, χ has a broad extent in ϑ.

This is the solution used for a trial function in the exterior region. For the case of small ε, or small E+F and H, the variational procedure then merely serves as a way to obtain the same solution as with matching, but without explicitly solving for $\delta\chi$ in $\vartheta\sim 1$, or the corrections to $\bar{\chi}_A$ in the outer region for small but finite coupling.

The trial function we will choose is

$$\chi_T = \begin{cases} \chi_c & \text{for } \vartheta \leqslant \vartheta_c \\ \chi_A & \text{for } \vartheta \geqslant \vartheta_c \end{cases} \tag{32}$$

with continuity at $\vartheta=\vartheta_c$ and $1 \ll \vartheta_c \ll \omega_s^2/\gamma^2$, say $\vartheta_c = (\omega_s/\gamma)^{1/2}$. The final dispersion relation will be independent of ϑ_c, as expected for well matched solutions. χ_A in the exterior includes both the average part, $\bar{\chi}_A$, and the small fluctuating parts.

C. Structure of V

It is useful to consider the structure of k(f), and estimate the size of its contributions. For simplicity we take $D_I = 0$ in the estimates here; the results for $-3/4 < D < 1/4$ are similar. $D_I = 0$ is not assumed in the analysis.

The most obvious feature is the propagator peak near k=0, where $\Phi(0) \sim 1$; thus the contribution to the integral in k(f) from the region near k=0 is $\sim\omega_s/\gamma$.

$\Phi(k)$ is also a sharply peaked function near $k = \pm 1, \pm 2, \ldots$. To see this, recall that $\kappa \sim (\partial\sigma/\partial\vartheta)\vartheta$ for large ϑ, where σ is a periodic function. From Eq. (29), we have $\kappa\chi \sim (\partial\sigma/\partial\vartheta)\exp(-M^{1/2}\vartheta\gamma/\omega_A)$. Since $\frac{\partial\sigma}{\partial\vartheta}$ is periodic and purely oscillatory, $\Phi(k)$ is peaked about nonzero integers. The width in ϑ of the integrand of Eq. (18) allows us to esimate that the peaks of Φ have width in $k \sim \gamma/\omega_A$ and height $\sim \omega_A/\gamma$. Thus, the contribution to the integral in k(f) from this region has magnitude ~ ω_A/γ. Since the propagator is nonresonant in this region, we call these contributions the nonresonant parts of k(f).

The contribution to the integral in k(f) from the regions away from k=0 and k = ±1, ±2 is only ~1. Thus, as $\gamma \to 0$, they are relatively negligible.

We now separate V into three pieces: 1) V_A, which includes the purely Alfvénic inertia term, nonresonant compressibility term, and line bending at large ϑ 2) $\delta\Delta W$, the net driving energy past β_c 3) $k_R(f)$, the resonant compressibility term

$$V = V_A + \delta\Delta W + k_R(f) \tag{33}$$

where

$$V_A = k_{NR}(f) + \frac{2}{J}\int_0^\infty d\vartheta J\left[-\gamma^2 \frac{|\nabla S|^2\rho}{B^2}\chi_T^2 - \left(\frac{|\nabla S|^2}{J^2B^2}\right)_c\left(\frac{\partial\chi_T}{\partial\vartheta}\right) + 2(J\kappa\rho')_c\chi_T^2\right] \tag{34}$$

$$\delta\Delta W = \int_{-\infty}^{+\infty} d\vartheta\left[\delta\left(\frac{|\nabla S|^2}{JB^2}\right)\left(\frac{\partial\chi_T}{\partial\vartheta}\right)^2 + 2\delta(J\kappa\rho')\chi_T^2\right] \tag{35}$$

and

$$k_R(f) = \frac{-4\Gamma\bar{p}}{\bar{J}^2}\frac{\gamma^2}{\omega_s^2}\int_{-k_0}^{-k_0}\frac{dk}{2\pi}\frac{|\Phi(k)|^2}{k^2+\gamma^2/\omega_s^2} . \tag{36}$$

$$k_{NR}(f) = \frac{-4\Gamma\bar{p}}{\bar{J}^2}\frac{\gamma^2}{\omega_s^2}\left(\int_{k_0}^{\infty} + \int_{-\infty}^{-k_0}\right)\frac{\Phi(k)\Phi(-k)}{k^2+\gamma^2/\omega_s^2} \tag{37}$$

where $\gamma/\omega_s \ll k_0 \ll 1$, say $k_0 = (\gamma/\omega_s)^{1/2}$.

The nonresonant contributions to k give the compressional augmentation of perpendicular inertia by roughly $1+2q^2$ found previously.[13]

D. Evaluation of Terms in V

For broad $\chi(\vartheta)$, $\Phi(k)$ is sharply peaked at nonzero integer values of k, due to the secularity in κ_ω. For large ϑ, $J\kappa_\omega \rightarrow -\vartheta(q'/2p')\partial\sigma/\partial\vartheta$. Define

$$\frac{q'}{2p'}\frac{\partial\sigma}{\partial\vartheta} = \sum_{n\neq 0} a_n e^{in\vartheta} . \tag{38}$$

Then near integer values of k

$$\Phi(k) \cong \sum_{n\neq 0} a_n \int d\vartheta\, e^{i(k+n)\vartheta}\, \vartheta\, \chi_T(\vartheta) = \sum_{n\neq 0} a_n S(k+n) \tag{39}$$

where $\quad S(k) = \int e^{ik\vartheta}\, \vartheta \chi_T(\vartheta)$. (40)

$S(k)$ is peaked with width $\Delta k \sim 1/\Delta\vartheta$, and $\Delta k \rightarrow 0$ as $\gamma/\omega_A \rightarrow 0$ [when $D_I > -3/4$; note Eq. (29)) Therefore as $\gamma/\omega_A \rightarrow 0$, k_{NR} is given by the integrals over these peaks,

$$k(f)_{NR} \equiv -\frac{4\bar{p}\Gamma\gamma^2}{\bar{J}\omega_s^2}\sum_n \frac{|a_n|^2}{n^2}\int \frac{dk}{2\pi} S(k)S(-k) \ . \tag{41}$$

The integral with S(k) is $\int \vartheta^2\chi^2(\vartheta)d\vartheta$. This can be combined with the perpendicular inertia term [first term in Eq. (16)] at large ϑ. The sum is

$$k(f)_{NR} + \gamma^2 I_\perp \cong \gamma^2 M q'^2 \langle\frac{\nabla\psi^2}{B^2}\rangle \int_{-\infty}^{+\infty} d\vartheta\vartheta^2\chi^2(\vartheta) \ . \tag{42}$$

Thus V_A becomes

$$V_A = \frac{2}{\bar{J}}\int_0^\infty d\vartheta J[-\gamma^2(|\nabla S|^2 M \frac{\rho}{B^2})_c \chi_T^2 - (\frac{|\nabla S|^2}{JB^2})_c(\frac{\partial\chi_T}{\partial\vartheta})^2 + 2(J\kappa_\omega)_c\chi_T^2] \ . \tag{43}$$

On integrating by parts, and using Eq. (32),

$$V_A = \frac{2}{\bar{J}}\int_0^{\vartheta_c} dJ\gamma^2 M' \frac{\rho|\nabla S|^2}{B^2} + \frac{2\chi_T}{\bar{J}}\frac{|\nabla S|^2\partial\chi_T}{JB^2\ \partial\vartheta}\Big|_{\vartheta_c-\varepsilon}^{\vartheta_c+\varepsilon} \ . \tag{44}$$

We now use the asymptotic behavior of χ_T as $\lambda\vartheta \to 0$, and of χ_c as $\vartheta\to\infty$, and the relations for the fluctuating parts. Neglecting terms small in γ/ω_A,

$$V_A = -2^{2-2\nu}\frac{\nu\Gamma(1-\nu)}{\Gamma(1+\nu)}\frac{q'^2\chi_\infty^2}{\bar{J}^2\langle\frac{B^2}{\nabla\psi^2}\rangle}\left(\frac{\sqrt{M}\gamma}{\omega_A}\right)^{2\nu} \tag{45}$$

independent of ϑ_c.

Now consider $k_R(f)$. For $D_I < 0$, the dominant contributions in $\Phi_T(k)$ come from $\vartheta \sim 1$. However, using the fact that χ_T nearly satisfies the equation for marginal stability, this $\Phi(k)$ can be found in terms of the asymptotic behavior of χ_T as $\vartheta \to \infty$; this allows us to find $\Phi(k)$ using Eq. (29). χ_T satisfies

$$H(\vartheta-\vartheta_c)\ \gamma^2\left(\frac{J\rho}{B^2} M|\nabla S|^2\right)_c \chi_T + \frac{\partial}{\partial\vartheta}\left(\frac{|\nabla S|^2}{JB^2}\right)_c \frac{\partial}{\partial\vartheta}\chi_T$$
$$+ 2(J\kappa_\omega)_c\chi_T = \delta(\vartheta-\vartheta_c)\ \frac{|\nabla S|^2}{JB^2}\frac{\partial\psi_T}{\partial\vartheta}\Bigg|_{\vartheta_c-\varepsilon}^{\vartheta_c+\varepsilon} \tag{46}$$

where H(x) is the Heaviside function; the delta function arises from the discontinuity in slope implied by Eq. (32).

As $\gamma \to 0$ the term on the right side become relatively negligible. Multiply Eq. (46) by $e^{-ik\vartheta}$ and integrate by parts, to give

$$\Phi(k) = \frac{-ik}{2p'} \int d\vartheta\ e^{ik\vartheta}\ \frac{|\nabla S|^2}{JB^2}\frac{\partial\chi_T}{\partial\vartheta} - \gamma^2 M\bar{J}q'^2\left<\frac{\rho}{B^2}|\nabla\psi|^2\right>_c \int d\vartheta\ e^{ik\vartheta}\vartheta^2\chi_T^2.$$

The integrand in the first term $\sim \vartheta^{-1/2+\nu}$. Thus for small k the dominant contribution comes from $\vartheta \gg 1$ and we can use the solution of Eq. (29). The main contribution from the second term also comes from large ϑ. The resulting integrals can be written in terms of hypergeometric functions. For $k \gg \gamma/\omega_A$, which is the relevant case when $\omega_s \ll \omega_A$, this simplifies to

$$\Phi(k) \cong \chi_\infty \sin[\frac{\pi}{2}(3/2-\nu)]\Gamma(3/2-\nu)k^{\nu-1/2} \frac{(-\frac{1}{2}-\nu+H)q'^2}{p'\bar{J}<B^2/\nabla\psi^2>} . \qquad (47)$$

For $\omega_s << \omega_A$ we thus have

$$k_R(f) = B(\nu)\left(\frac{q'\chi_\infty}{p'\bar{J}<B^2/|\nabla\xi|^2>}\right)^2 \frac{\Gamma\bar{p}}{\bar{J}^2}\left(\frac{\gamma}{\omega_s}\right)^{2\nu} \qquad (48)$$

where $B(\nu) = 2\sin[\frac{\pi}{2}(3/2-\nu)]^2[\Gamma(3/2-\nu)(-1/2-\nu+H)]^2/\sin(\nu\pi)$. (49)

E. Dispersion Relation

We finally have

$$-\delta\Delta W = V_A + k_R(f)$$

$$= \frac{\chi_\infty^2}{\bar{J}^2}\frac{q'^2}{<|\nabla\psi|^2>}\left[A(\nu)\left(\frac{\sqrt{M}\gamma}{\omega_A}\right)^{2\nu} + \frac{B(\nu)q'^2\bar{p}\Gamma}{p'^2\bar{J}^2<B^2/|\nabla\psi|^2>}\left(\frac{\gamma}{\omega_s}\right)^{2\nu}\right] \qquad (50)$$

where $A(\nu) = 2^{2-2\nu}\,\nu\Gamma(1-\nu)/\Gamma(1+\nu)$. (51)

This expression depends only on simple equilibrium parameters, with one exception: the ratio $\delta\Delta W/\chi_\infty^2$. The numerical evaluation of this requires χ_c, the solution of the second order Euler differential equation to determine marginal stability.

The ratio of the terms on the right gives the relative importance of modified Alfvénic physics and resonant sonic physics. The ratio does not depend on details of χ_c, but only on simple equilibrium quantities.

Nonresonant compressibility effects have augmented the purely Alfvénic contribution by M^{ν}. Note that the coefficient multiplying the resonant term is $\sim \varepsilon^{1-\nu}$. Recall $\nu \equiv \sqrt{1-4D_I}$. Fractional powers of ε are not small for realistic parameters. For the model equilibrium in the next section, the resonant terms are found to be as important as the nonresonant ones for realistic parameters. Note, however, that as the magnetic axis is approached the resonant terms become relatively unimportant, because of the behavior of q', p' and $\nabla\psi$.

IV. Numerical Results

Here we numerically solve Eqs. (2)-(3) to examine compressibility effects further from marginal stability than in Sec. III.

We use the model equilibrium with circular flux surfaces of Connor et al.,[13] with an additional constant average curvature term to give the effects of D_I. R_0 and B_T are the major radius and toroidal field on axis, r_0 is the minor radius, $L_\perp$ the pressure scale length, q is the safety factor.

$$\varepsilon = L_\perp/R_0$$

$$\alpha = \frac{2q^2}{B_T^2}\frac{P}{\varepsilon} = \varepsilon\beta_p$$

$$\hat{s} = \partial(\ln q)/\partial(\ln r)$$

$$J = qR_0/B_T \tag{52}$$

$$\kappa_\omega = \frac{q}{R_0 r_0 B_T}\left[\cos\vartheta - \sin\vartheta(\hat{s}\vartheta - \alpha\sin\vartheta) + \frac{\hat{s}^2 D_I}{\alpha}\right] \equiv \frac{q}{R_0 r_0 B_T}\kappa_N$$

$$|\nabla S|^2 = \left(\frac{q}{r_0}\right)^2 [1 + (\hat{s}\vartheta - \alpha\sin\vartheta)^2] \equiv \left(\frac{q}{r_0}\right)^2 |\nabla S|_N^2$$

$$\omega_A^2 = \rho q^2 R_0^2/B_T^2$$

$$\omega_s^2 = (\alpha\varepsilon/2q^2)\omega_A^2 ,$$

Thus Eqs. (2)-(3) can be written

$$\frac{\gamma^2}{\omega_A^2}|\nabla S|_N^2\,\chi = \frac{\partial}{\partial\vartheta}|\nabla S|_N^2 \frac{\partial}{\partial\vartheta}\chi + \kappa_N(\alpha\chi + 2q^2 f')$$

$$\frac{\partial^2 f'}{\partial\vartheta^2} - \frac{\gamma^2}{\omega_s^2} f' = 2\frac{\gamma^2}{\omega_A^2}\kappa_N\chi , \tag{53}$$

where $f = (Bq/R_0 r_0) f'$.

Solutions of γ versus α are shown in Fig. (2)-(3) for $\hat{s}=.7$, $\varepsilon = .07$ and $D_I = 0$ and $-.3$. Also shown are solutions to the second order system corresponding to Eq. (9) which neglects all compression effects. The growth rates are indeed sharply reduced.

The power law dependence of γ on $\alpha-\alpha_c$, $\gamma^{2\nu} = C(\alpha-\alpha_c)$ agrees very well with Eq. (50) near α_c.

The coefficient C can also be found from Eq. (50), using a numerically obtained χ_c. This result is also plotted and the agreement is quite good. (Recall an expansion was made in Eq. (47) for $\omega_s^2/\omega_A^2 \sim \varepsilon$, even for E+F = 0 and H=0.)

Evaluation of the terms in the analytical dispersion relation shows that the resonant compressibility term is nearly as large as the nonresonant one, and each are larger than the purely Alfvénic term by roughly a factor of 2.

Also plotted is the point α_c' (corresponding to β_c' in the discussion in Sec. I.A) where $\Delta W < 0$ when $\xi_\parallel = 0$ (given by taking $f' = 2\omega_s^2\kappa_N\chi/\omega_A^2$). Surprisingly, the analytic dispersion relation is still reasonably accurate for $\alpha \sim \alpha_c$.

V. KINETIC FORMULATION

A. Kinetic Equations

We now examine these effects in a kinetic regime. The ballooning equations of Antonsen and Lane are used. We will rewrite these equations in a form more appropriate for MHD like perturbations. It is then possible to write a variational form similar to Eq. (16), for the fully kinetic case. Since our concern here is with compressibility effects on nondissipative ballooning modes, we will make numerous simplifying approximations in its derivation. We note that the form can be greatly generalized to relax these (to be presented in the future; also, Berk et al.[17] have obtained a variational form similar to the one here).

The kinetic equations are in terms of the fields $A_{\parallel}$, Φ, $\delta B_{\parallel}$ and the distribution function h in terms of the energy E and magnetic moment μ. It is convenient to define χ and φ by

$$A_{\parallel} = \frac{-i}{JB}\frac{\partial \chi}{\partial \vartheta} \tag{54}$$

$$\varphi = \Phi - \omega\chi .$$

χ will play a role similar to the stream function in the MHD. We take the equilibrium distribution function F_0 to be a Maxwellian with density and temperature gradients, $F_0 = n(\psi)\exp[E/T(\psi)]$. Also, define $f_s(E,\mu)$, which is the kinetic equivalent of f in Eq. (11),

$$h_s(E,\mu) = \frac{q_s}{T_s}(\omega-\omega_{*s})F_{0s}J_0\chi + f_s(E,\mu) \tag{55}$$

where q_s and T_s are the charge and temperature of species s, $\omega_{*s} = -T_s B\times\nabla S\cdot\nabla n[1+\eta(E/T-3/2)]/nB^2_{q_s}$, $J_0 = J_0(|\nabla S|\rho_s)$, $J_1 = J_1(|\nabla S|\rho_s)$, $\rho_s = v_\perp m_s/q_s B$, and $\eta = (T/n)dT(\psi)/dn(\psi)$. The kinetic equation for f_s is

$$-i(\omega-\omega_d)f_s + C(f_s) + \frac{v_\parallel}{JB}\frac{1}{JB}\frac{\partial}{\partial\vartheta}f_s =$$

$$\frac{-iq_s}{T_s}(\omega-\omega_{*s})[\omega_d J_0\chi + J_0\varphi - \frac{iv_\parallel}{JB}\frac{\partial}{\partial\vartheta}J_0 + \frac{v_\perp}{k_\perp}J_1\delta B_\parallel] \ , \qquad (56)$$

where $C(f_s)$ is the collision operator, and $\omega_d \equiv \nabla S\cdot\hat{b}\times(m_s v_\parallel^2\hat{b}\cdot\nabla\hat{b}+\mu\nabla B)/m_s\Omega_s$. Quasineutrality gives

$$0 = -\sum_s \frac{q_s^2}{T_s}\varphi + \sum_s \frac{q_s^2}{T_s}\int dv\ [(J_0^2-1) - \frac{\omega_{*s}}{\omega}J_0^2]F_0\chi + \sum_s q_s\int dv\ J_0\ f_s \ ,$$

where $\int dv\ A = 2\pi B/m_s^2\int_0^\infty dE\int_0^{E/B}d\mu\ \frac{A_+ + A_-}{\sqrt{E-\mu B}}$. The radial component of Ampere's Law is

$$\delta B_\parallel = \chi\sum_s \frac{q_s^2}{T_s}\int dv\ (\omega_{*s}-\omega)\frac{v_\perp}{VS|}J_1 J_0 F_0 - \sum_s q_s\int dv\ \frac{v_\perp}{|\nabla S|}J_1 f_s \ .$$

The parallel component of Ampere's Law relates χ and the parallel current, which is found by multiplying the kinetic equation by $q_s J_0$, taking $\int dv$, and eliminating the density moment with quasineutrality. Neglecting the kink driving term,

$$0 = \frac{1}{J}\frac{\partial}{\partial\vartheta}\frac{|\nabla S|^2}{B^2 J}\frac{\partial}{\partial\vartheta}\chi + \sum_s \frac{q_s^2}{T_s}\int dv(\omega-\omega_{*s})\omega_d J_0^2 F_{0s}$$

$$-\ (\omega\chi+\varphi)\sum_s \omega\frac{q_s^2}{T_s}\int dv[(J_0^2-1) - J_0^2\frac{\omega_{*s}}{\omega}]F_0$$

$$-\ \delta B_\parallel \sum_s q_s^2 T_s \int dv\ (\omega_{*s}-\omega)\frac{v_\perp}{k_\perp} J_1 J_0 F_0 + \sum_s q_s \int dv\ (\omega_d J_0 + \frac{i v_\parallel}{JB}\frac{\partial}{\partial\vartheta} J_0) f_s\ . \quad (57)$$

These equations are simplified by neglecting f_e and taking $\nabla S\rho_s << 1$.

Neglecting f_e is an enormous simplification because it allows φ and $\delta B_\parallel$ to be obtained as algebraic, local functions of χ and velocity integrals of f_i. Physically, it corresponds to taking the electron response to be adiabatic, with the inductive electric field included. It is well justified in several circumstances. Recall that we are considering modes with $\omega \sim v_{ti}/qR$, where v_{ti} is the thermal ion speed. Thus the passing electron response f_e is smaller than f_i by v_{ti}/v_{te}, and its neglect is valid. However, the trapped electron response f_e^t could be of order f_i. f_e^t is smaller than f_i if the electron Coulomb collisional detrapping rate, ν_{eff}^e, greatly exceeds ω. It is still possible to have nearly collisionless ions, $\nu_{eff}^i < \omega$, since $\nu_e/\nu_i \sim \sqrt{m_i/m_e}$. Note that this rapid electron detrapping ordering holds for $\omega \sim v_{ti}/qR$ unless the plasma is very deeply into the banana regime, $\nu_{eff}^e/qv_{te} \lesssim \sqrt{m_e/m_i}$. (Of course, electron dissipative effects at high ϑ lead to resistive ballooning modes, but these are beyond our present scope.) The electron trapped response can also be neglected in the collisionless case if the fraction of trapped particles is small, or if $T_e/T_i << 1$, since the contribution of trapped electron pressure to Eq. (57) is then negligible anyway.

The small gyroradius approximation proceeds by noting that $\omega_* \sim k_\perp \rho_i \; v_{ti}/L_\perp$, where $L_\perp$ is the perpendicular pressure scale length. We then neglect terms of order $k_\perp^2 \rho_i^2$. We keep FLR effects of order $\omega_*/\omega \sim k_\perp \rho_i L_\parallel / L_\perp$, where $L_\parallel$ is a parallel scale length. Small $k_\perp \rho_i$ and $\omega \sim \omega_*$ is consistent if $L_\parallel >> L_\perp$.

After eliminating φ and $\delta B_\parallel$, the result is

$$\frac{1}{J}\frac{\partial}{\partial\vartheta}\frac{|\nabla S|^2}{JB^2}\frac{\partial}{\partial\vartheta}\chi + 2\kappa_\omega p'\chi +$$

$$\{\omega[\omega-(1+\eta)\omega_*] + \frac{\beta_i}{2}\omega_*[\omega-(1+2\eta)\omega_*]\}\frac{|\nabla S|^2}{B^2}\chi - T_i\int dv\kappa_\omega^k = 0 \tag{58}$$

$$-i(\omega-\omega_d)f_i + \frac{i(\omega-\omega_{*i})}{1+\frac{T_i}{T_e}}\frac{F_0}{n_0}\int dv f_i + (\omega-\omega_{*i})\frac{mv_\perp^2}{2B^2}F_0\int dv\,\frac{1}{2}\frac{mv_\perp^2}{T}f_i$$

$$+\frac{v_\parallel}{JB}\frac{\partial f_i}{\partial\vartheta} + C(f_i) = iq(\omega-\omega_{*i})\;\chi\kappa_\omega^k F_0 \;, \tag{59}$$

where

$$\kappa_\omega^k = \kappa_\omega\frac{m(v_\parallel^2+v_\perp^2/2)}{T_i}\;,\;\omega_{*n} = -T_iB\times\nabla S\cdot\nabla n/nB_{qi}^2$$

and β_i is the ion β. The terms in Eq. (59) $\sim\int f_i dv$ and $\int mv_\perp^2 f_i dv$ arise from eliminating φ and $\delta B_\parallel$, respectively. Physically, these terms give the contribution of electron pressure to ion acoustic waves, and magnetosonic corrections to ion acoustic waves, respectively.

There are obvious similarities between Eqs. (4), (11)-(12) and Eqs. (58)-(59). Instead of a fluid propagator, f_i is now determined by a kinetic propagator. However, f is still driven by a term proportional to $\kappa_\omega \chi$, and it enters the equation for χ as $\kappa_\omega f$.

We now examine kinetic modifications of the results in Sec. III in several regimes.

B. MHD Regime with Landau Damped Ions.

Here we examine the MHD-like case with $\omega \gg \omega_*$, but with negligible $C_i(f_i)$. We consider small $\varepsilon \sim \beta$. We consider frequencies above the bounce frequency $\sim \varepsilon^{1/2} \omega_s$, so we may neglect trapped ion and bounce resonance effects. Also, since ε is small, we neglect ϑ variations in 1/JB and the ϑ variations of $v_\parallel$. Of course these variations are large for trapped particles, but with $\omega > \omega_b$ the $v_\parallel$ term is relatively unimportant for them anyway. Fourier expanding in ϑ, as in Eq. (18), the above limits give

$$-i\left(\omega - \frac{v_\parallel}{qR} k\right) f_i = \frac{+i\omega m_i (v_\parallel^2 + v_\perp^2/2)}{T_i} \frac{F_0}{J} \Phi(k) \qquad (60)$$

with $\Phi(k)$ from Eq. (18).

The dispersion relation can then be written in the variational form

$$-\gamma^2 \frac{1}{J} \int d\vartheta J \frac{\rho}{B^2} |\nabla S|^2 \chi^2 + \frac{1}{J} \int d\vartheta J [-\frac{|\nabla S|^2}{J^2 B^2} (\frac{\partial \chi}{\partial \vartheta})^2 + 2p' \kappa_\omega \chi^2] = K_k(f) \tag{61}$$

$$K_k(f) = \frac{p_0}{J^2} \int \frac{dk}{2\pi} \Phi(k)\Phi(-k) G_k(k)$$

$$G_k(k) = [-\Omega Z_2(\Omega) + \Omega^2 Z_1(\Omega)^2/[1 + \frac{T_i}{T_e} + \Omega Z(\Omega)]]/(1 + \frac{T_e}{T_i})$$

$$Z_2(\Omega)/(1 + \frac{T_e}{T_i}) = \frac{1}{\sqrt{\pi}} \int ds\ e^{-s^2} (4s^4 + 4s^2 + 2)/(s - \Omega)$$

$$Z_1(\Omega) = \frac{1}{\sqrt{\pi}} \int ds\ e^{-s^2} (2s^2 + 1)/(s - \Omega)$$

$$Z(\Omega) = \frac{1}{\sqrt{\pi}} \int ds e^{-s^2}/(s - \Omega)$$

and $\Omega = \omega | qR/v_{ti} k|$ with $v_{ti} = \sqrt{2T_i/m_i}$.

Note the similarity between Eqs. (61) and (19); clearly the only difference is that the fluid propagator, $\gamma^2/(\omega_s^2 k^2 + \gamma^2)$, has been replaced by the kinetic propagator, which includes Landau resonance effects. As might be expected, as $T_e/T_i \to 0$ the G_k approaches the fluid propagator, since then ion kinetic effects are negligible. Numerical evaluation of $G_k(\Omega)$ when $Re(\Omega) = 0$ shows that, for $T_e/T_i > 0$, it is larger than the fluid propagator (which can also be written in terms of Ω and T_i/T_e). G_k also increases monotonically with Ω. Thus, the growth rates in the kinetic regime are less than the fluid values. This reduction is particularly marked when $\gamma/\omega_s \ll 1$.

We can again separate the source of contributions to $K_k(f)$ into two regions of k for $\omega/\omega_s < 1$; a region near k=0, where G_k is peaked, and regions near $k = \pm 1, \pm 2, \ldots$, where Φ is peaked.

The contributions from non-zero integer k are substantially altered. The fluid propagator here is $\sim\gamma^2/\omega_s^2 k^2$. Because of resonant particle interactions, the kinetic propagator is $\sim\gamma/\omega_s k$, bigger by the large factor ω_s/γ. Thus in the kinetic case, for $\gamma/\omega_s \to 0$, the contributions near from $k = \pm 1, \pm 2\ldots$ dominate those from $k \sim \omega_s/\gamma$. We thus neglect the latter in what follows.

As previously, we need the large ϑ behavior of χ, which we find from two space scale analysis. Thus, $f = \bar{f} + \tilde{f}$ and $\chi = \bar{\chi} + \tilde{\chi}$. Again $\tilde{\chi} << \bar{\chi}$, and the contributions from $\bar{f}$ in the exterior are relatively small by ε. $\tilde{f}$ satisfies

$$-i\omega\tilde{f} + \frac{v_{\parallel}}{qR_0}\frac{\partial\tilde{f}}{\partial\vartheta} = \frac{-i\omega m(v_{\parallel}^2 + v_{\perp}^2/2)}{T_i\bar{J}}\,\vartheta\bar{\chi}\sum_n a_n e^{in\vartheta} \tag{62}$$

with a_n given by Eq. (34). The average of the term in the equation for χ, Eq. (58), is

$$a_i \int dv\, \overline{\tilde{\omega}_{\kappa}\tilde{f}_i} = \frac{\bar{P}}{\bar{J}^2}\,\bar{\chi}\vartheta^2 \sum_n a_n^2 G_k(\Omega_n) \tag{63}$$

where $\Omega_n = \omega|qR/nv_{ti}|$.

Since this term is proportional to ϑ^2, computation of the dispersion relation proceeds as in Sec. III. Equation (63) is used to determine $\bar{\chi}$ in analogy with Eq. (29). Evaluation of the contribution from the peaks proceeds as in Sec. IIID — the only difference is that the factor M is replaced by a kinetic result.

We obtain

$$\left(\frac{-\delta\Delta W \bar{J}^2 \left\langle \frac{B^2}{|\nabla\psi|^2} \right\rangle}{\chi_\infty^2 q'^2 A(\nu)}\right)^{1/\nu} = \frac{\gamma^2}{\omega_A^2} + \frac{p}{q'^2} \left\langle \frac{B^2}{|\nabla\psi|^2} \right\rangle \sum_n |a_n|^2 G_k(\Omega_n) \ . \tag{64}$$

For $\gamma/\omega_s << 1$, the second term is $\sim q^2\gamma\omega_s/\omega_A^2$; thus the kinetic compressibility terms dominate the purely Alfvenic term when $\gamma/\omega_s < 1$. Again, recall that when $\gamma \sim \omega_b << \omega_s$ bounce resonance effects (neglected here) must be included.

VI. Finite Larmor Radius Effects

The results of Sec. III–V show that the growth rates are much less than ω_A significantly past β_c. Thus, the growth rate can be the same size as the diamagnetic frequency for surprisingly low mode numbers. For a hydrogen plasma,

$$\frac{\omega_*}{\omega_A} = \frac{\alpha n}{17(1+T_e/T_i)} \left(\frac{20\text{cm}}{r_0}\right)\left(\frac{n_i}{10^{14}\text{cm}^{-3}}\right)^{-1/2}$$

where n is the toroidal mode number and α is given by Eq. (52). For PDX and Doublet III parameters, and for $\beta/\beta_c = 1.1$ (using the results of Sec. IV), this indicates $\gamma \sim \omega_*$ when $n \sim 2$–5. Previous incompressible analyses show that stability is achieved for $\omega_* > 2\gamma_{MHD}$. It is thus important to consider the effects of ω_* with compressibility.

Here we show that compressibility effects can nullify the stabilizing effects of ω_*. We begin by neglecting temperature gradients. First we consider a fluid ion limit with strong coupling to parallel compressibility, $\omega << \omega_s$. The destabilization arises from the resonance in the fluid propagator. We then analytically consider a kinetic case with $\omega \lesssim \omega_s$ and collisionless parallel dynamics but with small shear or very small aspect ratio. Then we consider a limit where parallel compressibility can be neglected, $\omega >> \omega_s$, which manifests a different FLR destabilization mechanism. We then consider temperature gradients. We find that the Alfvén continuum has frequencies with positive imaginary parts, when $\omega \sim \omega_s$. This could lead to instabilities below β_c. The question of unstable eigenmodes below β_c is then hueristically discussed.

A. Fluid Ion Case with Parallel Compressibility.

For simplicity we take C(f) to be a Krook operator which conserves particles and ion momentum, and we neglect ion viscous effects. With $C >> \omega,\omega_s$ to lowest Eq. (59) gives $f_i = N(\vartheta)f_M + v(\vartheta)v_\parallel f_0$, for arbitrary $N(\vartheta)$ and $V(\vartheta)$. These functions are obtained by taking momoents of Eq. (59). For small ε, the FLR modified versions of Eq. (2), (11)-(12) become, (for $T_e=T_i$ and neglecting temperature gradients)

$$-(\omega-\beta_i\omega_{*i}/2)(\omega-\omega_{*i}) \frac{\rho}{B^2} |\nabla S|^2\chi = \frac{\partial}{\partial\vartheta} \frac{|\nabla S|^2}{JB^2} \frac{\partial\chi}{\partial\vartheta} + 2\kappa_\omega[p'(\psi)\chi+f] \qquad (65)$$

$$\frac{\partial}{\partial\vartheta} \frac{1}{JB^2} \frac{\partial f}{\partial\vartheta} + \rho\omega(\omega+\omega_{*i}) \frac{(B^2+p)}{B^2 p} = -2\omega(\omega-\omega_{*i})\rho J\kappa_\omega \qquad (66)$$

(note $\Gamma=1$ for this collision operator).

This gives the FLR modified form of Eqs. (16) and (19),

$$(\omega-\beta_i\omega_{*i}/2)(\omega-\omega_{*i}) \frac{1}{J}\int d\vartheta J \frac{\rho}{B^2}|\nabla S|^2\chi^2 + \frac{1}{J}\int d\vartheta J\left[\frac{-|\nabla S|^2}{J^2B^2}\left(\frac{\partial\chi}{\partial\vartheta}\right)^2 + 2\rho'\kappa_\omega\chi\right]$$

$$+ k_f^{FLR}(f) = 0 \qquad (67)$$

$$k_f^{FLR}(f) = \frac{4\bar{p}}{\bar{J}^2}\frac{\omega(\omega-\omega_{*i})}{\omega_s^2}\int_{-\infty}^{+\infty}\frac{\Phi(k)\Phi(-k)}{k^2 - \frac{\omega(\omega+\omega_{*i})}{\omega_s^2}} . \tag{68}$$

For $\omega \sim \omega_* \ll \omega_s$ and $\omega_s \ll \omega_A$ the procedure leading to Eq. (50) can be used to find the dispersion relation. Taking $\omega_{*i} > 0$ for definiteness,

$$\delta\Delta W = V_A^{FLR} + K_f^{FLR} = \frac{\chi_\infty^2 q'^2}{\bar{J}^2 \langle \frac{B^2}{|\nabla\psi|^2} \rangle}\{A(\nu)\left(\frac{M\omega(\omega_{*i}-\omega)}{\omega_A^2}\right)^\nu$$

$$+ e^{i\pi\nu}\frac{B(\nu)q'^2\bar{p}}{p'^2\bar{J}^2\langle B^2/|\nabla\psi|^2\rangle}\frac{(\omega-\omega_{*i})}{(\omega+\omega_{*i})}\left[\frac{-\omega(\omega_{*i}+\omega)}{\omega_s^2}\right]^\nu\} . \tag{69}$$

The possible singularity in the denominator of Eq. (68) is resolved by the Landau prescription.

When the resonant contribution is negligible, the dispersion relation can be written

$$-\gamma_{MHD}^2 = \omega(\omega-\omega_{*i})$$

where γ_{MHD}^2 is the growth rate for $\omega_{*i} = 0$. As usual, this implies stability for $\gamma_{MHD}^2 < \omega_{*i}^2/4$. Note that, neglecting the resonant term, the non-resonant modifications enhance the stability influence of ω_* because the MHD growth rate is reduced by a factor M^ν.

Let us consider the resonant contribution as a perturbation on a case where $0 < \gamma_{MHD}^2 < \omega_{*i}^2/4$. To lowest order ω is given by Eq. (69), $\omega_0 = \omega_{*i}/2 \pm \Delta$, where $0 < \Delta < \omega_{*i}/2$. With the perturbation, $\omega = \omega_0 + \delta\omega$, where

$$-\delta\omega \frac{\partial V_A^{FLR}}{\partial\omega} = 2\nu\delta\omega\left(\omega_0 - \frac{\omega_*}{2}\right)\left(\gamma_{MHD}/\omega_A\right)^{2\nu}$$

$$= e^{i\pi\nu} \frac{B(\nu) q'^2 \bar{p}}{p'^2 \bar{J}^2 \left\langle \frac{B^2}{|\nabla\psi|^2} \right\rangle} \left(\frac{\omega_0 - \omega_{*i}}{\omega_0 + \omega_*}\right)\left(\frac{\omega_0(\omega_{*ii} + \omega_0)}{\omega_s^2}\right)^{\nu} . \tag{70}$$

For $0 < \nu < 1$ this implies instability for the root $\omega_0 > \omega_{*i}/2$. Stability now occurs at $\delta\Delta W = 0$, and there is no FLR stabilization. For realistic aspect ratio and $\omega_{*i} \sim \gamma_{MHD} \sim \omega_s$ the resonant term is not small. The above result then indicates $\mathrm{Im}(\delta\omega) \sim \gamma_{MHD}$; i.e., the growth rate is not dramatically reduced. This is seen by numerically solving Eqs. (65)-(66) with the same geometrical coefficients as in Sec. IV. We take $\beta/\beta_c = 1.04$ and increase ω_{*i}. The results are shown in Fig. 4. Stability is not achieved for $\omega_*/2 > \gamma_{MHD}$ (γ_{MHD} is γ when $\omega_* = 0$). In these runs, ω_* was increased beyond ω_s without achieving stability. Equation (69) is not valid in this regime; we consider $\omega > \omega_s$ in part C.

Note that these figures show $\omega - \omega_* \to 0$ when $\omega(\omega+\omega_*)/\omega_s^2 \simeq 1$. This is predicted by Eq. (68), given the structure of $\Phi(k)$ and the denominator singularity in $k_f^{fLR}(f)$.

B. FLR Effects with Collisionless Parallel Ions

Now consider the collisionless case with $\omega \sim \omega_*$ without temperature gradients. Equation (61) still holds, except γ^2 is replaced by $-\omega(\omega-\omega_{*i})$ in the Alfvénic term, and that the propagator is replaced by

$$G_K^{FLR}(\Omega) = \frac{(1-\frac{\omega_*}{\omega})}{1+\frac{T_e}{T_i}}\left[-\Omega Z_2(\Omega) + \frac{(1-\frac{\omega_*}{\omega})\Omega^2 Z_1(\Omega)^2}{1+\frac{T_i}{T_e}+(1-\frac{\omega_*}{\omega})\Omega Z(\Omega)}\right] .$$

An analytic dispersion relation can be derived as in Sec. IVB, Contributions from k~0 are again neglected. This is justified for $\omega << \omega_s$ as in Sec. VB. The regime $\omega \sim \omega_s$ is also of interest, however. Neglect of the contributions from k~0 is justified in the limit of extremely small ε, or as the magnetic axis is approached. In these limits, more detailed estimates of the kind used in Sec. IIIC allow us to keep only the contribution in the integral in K(f) from k near ±1, ±2,... . We obtain the FLR modified version of Eq. (64)

$$\left[\frac{-\delta\Delta W \bar{J}^2 \langle\frac{B^2}{|\nabla\psi|^2}\rangle}{\chi_\infty^2 q'^2 A(\nu)}\right]^{1/\nu} + \frac{\omega(\omega_*-\omega)}{\omega_A^2} + \frac{p}{q'^2}\langle\frac{B^2}{|\nabla\psi|^2}\rangle \sum |a_n|^2 G_k^{FLR}(\Omega_n) \equiv D=0 \qquad (71a)$$

It is convenient to write the term containing $\delta\Delta W$ in terms of γ_{MHD}, which can be done by using Eq. (71), but with the fluid propagator. Antonsen has obtained a similar result for the ideal MHD case of small shear.[14] Furthermore, if all frequencies are normalized to $\varepsilon^{1/2}\omega_A$, aspect ratio dependences cancel out. For the model geometrical coefficients used by Connor et al.,[13] we finally obtain

$$\gamma'^2_{MHD} + \frac{2q^2\gamma'^2_{MHD}}{1 + \frac{2q^2}{\alpha}\gamma'^2_{MHD}} = -\omega'(\omega'-\omega'_*) + \frac{\alpha}{4} G_k(\Omega') \tag{71b}$$

where $\omega' = \omega/\omega_A\varepsilon^{1/2}$, $\omega'_* = \omega_{*i}/\omega_A\varepsilon^{1/2}$, $\gamma'_{MHD} = \gamma_{MHD}/\omega_A\varepsilon^{1/2}$, and $\Omega' = q\omega'\sqrt{(1+T_e/T_i)}/\alpha$. The first and second terms on each side of Eq. (73) are the pure Alfvénic and compressional terms.

For the case $T_e/T_i \to 0$, a Nyquist analysis on D demonstrates that instability results for $\delta\Delta W > 0$, for any ω_*. Since the $D\to\omega^2$ as $\omega\to\infty$, the number of roots in the upper half plane is equal to the number of encirclements plus one. As $\omega \to \pm\infty$, $D\to+\infty$ along the real axis. Im(D)=0 implies $\mathrm{Im}(G_k^{FLR}) = 0$, which occurs only when $\omega = \omega_{*i}$. The last two terms then vanish. If the plasma is MHD unstable, Re(D) > 0, so there are no encirclements and thus are unstable root. Thus, ω_* effects do not stabilize an MHD unstable mode. Numerical evaluation of Eq. (73) is shown in Fig. (5) and (6); a scan of increasing ω_* is shown for γ'_{MHD} = .1 and .5. The growth rate is initially smaller for $\omega_*=0$, as discussed in Sec. IVB. Increasing ω_* eventually leads to a slight increase in the growth rate above γ_{MHD}, however. Note that the maximum growth rate is always attained when $\omega'_* \cong \omega'\sim 1$.

C. Fluid Ions without Parallel Compression

We now consider the case where $\omega_* > \omega_s$. Then the parallel dynamics are irrlevant in Eq. (59). The collisionless and collisional cases are then similar; for definiteness we take the collisional case, Eq. (66). The mode equation for $\omega \sim \omega_* >> \omega_s$ is similar to that considered by Hastie and Hasketh[6] and Chen[7]

$$[\omega(\omega_{*i}-\omega) \frac{\rho}{B^2} |\nabla S|^2 + 4 \frac{\omega-\omega_{*i}}{\omega+\omega_{*i}} (\frac{B^2 p}{B^2+p})\kappa_\omega^2]\chi = \frac{\partial}{\partial\vartheta} \frac{|\nabla S|^2}{JB^2} \frac{\partial}{J\vartheta} \chi + 2\kappa_\omega p'(\psi)\chi \ . \quad (72)$$

The compressibility term has been modified by the factor $(\omega-\omega_{*i})/(\omega+\omega_{*i})$. For a mode with $0 < \mathrm{Re}\omega < \omega_{*i}$, this changes the sign of the compressibility term from stabilizing to destabilizing. This was noted by Tang et al.[2] This is an important effect in the shaded region of Fig. 1.

For $\omega < \omega_A$ the dispersion relation for this case can be found by a procedure similar to that used in Sec. II for the Alfvénic terms. The κ_ω^2 term is similar to the $|\nabla S|^2$ term, since $\kappa_\omega^2 \rightarrow G(\vartheta)^2\vartheta^2$ at large ϑ, for some periodic function $G(\vartheta)$. Thus,

$$[\frac{\delta\Delta W}{\chi_\infty^2} \frac{\bar{J}^2 \langle B^2/|\nabla\psi|^2\rangle}{q'^2 A(\nu)}]^{1/\nu} + \frac{\omega_{*i}-\omega}{\omega+\omega_{*i}} \frac{\langle \frac{B^2 p}{B^2+p} G^2 \rangle}{\rho \langle \frac{|\nabla S|^2}{B^2} \rangle} = \frac{\omega(\omega_{*i}-\omega)}{\omega_A^2} \ . \quad (73)$$

The dispersion relation can be written as a cubic equation in ω with real coefficients. For stability, all roots must be real, since one member of a conjugate pair must have $\mathrm{Im}(\omega) > 0$. Without the compressibility term, there is a root pair $\omega = \omega_{*i}/2 \pm \Delta$. The compressibility term is positive for $0 < \omega < \omega_{*i}$. Consider a case which is stabilized by FLR when the compressibility term vanishes. As the compressibility term is increased, the right-hand side must increase, which implies that the roots move closer together. When the left side exceeds $\omega_{*i}^2/4$, which occurs for sufficiently large ε, there is no pair of real roots so instability results.

But for given ε, it can similarly be shown that there is stability for sufficiently large ω_*. For $\beta_c < \beta \lesssim \beta_c'$, the necessary ω_* for stability is of order $\varepsilon^{1/2}\omega_A$. This is of order ω_s in a nominal ordering $\beta \sim \varepsilon$, so the neglect of parallel compressibility for such ω_* is questionable in general. (Note that a subsidiary ordering of large safety factor q gives a rigorous justification.)

If $\omega_* \gg \varepsilon^{1/2}\omega_A$ then $\omega \sim \omega_* \gg \omega_s$ and parallel compressibility can again be ignored; the above analysis then implies stability. Cheng has numerically examined this case without parallel dynamics. Drift resonances at large ϑ, (where $\nabla s \rho_i \sim 1$), can still give instability when $\omega_* \gg \varepsilon^{1/2}\omega_A$. However, these effects are exponentially small for small ε.

D. Temperature Gradient Effects on the Continuum

We take the average of Eq. (58). We use the analysis of part B to compute the average of the last term, but keep temperature gradients. At sufficiently large ϑ, we get

$$\frac{\partial}{\partial\vartheta} \vartheta^2 \frac{\partial}{\partial\vartheta} \bar{\chi} + k_0^2 \vartheta^2 \bar{\chi} = 0 \tag{74}$$

where

$$k_0^2 = \frac{\omega[\omega-\omega_{*n}(1+\eta)]}{\omega_A^2} - \frac{p}{q'^2} < \frac{B^2}{|\nabla\psi|^2} > \sum |a_n|^2 \, G_k^T(\Omega) \tag{75}$$

where

$$G_k^T(\Omega) = -\Omega\{(1 - \frac{\omega_{*n}}{\omega})Z_2(\Omega) - \eta \frac{\omega_{*n}}{\omega} Z_2^T(\Omega)]$$

$$+ \frac{\Omega^2[(1 - \frac{\omega_{*n}}{\omega})Z_1(\Omega) - \eta \frac{\omega_{*n}}{\omega} Z_1^T(\Omega)]^2}{1 + \frac{T_i}{T_e} + \Omega[(1 - \frac{\omega_{*n}}{\omega})Z(\Omega) - \eta \frac{\omega_{*n}}{\omega} Z^T(\Omega)]}) \tag{76}$$

with

$$Z_2^T(\Omega) = \frac{1}{\sqrt{\pi}} \int \frac{ds e^{-s^2}}{s-\Omega} (4s^6+2s^4+4s^2+3)$$

$$Z_1^T(\Omega) = \frac{1}{\sqrt{\pi}} \int \frac{ds e^{-s^2}}{s-\Omega} (2s^4+1/2)$$

$$Z^T(\Omega) = \frac{1}{\sqrt{\pi}} \int \frac{ds e^{-s^2}}{s-\Omega} (s^2-1/2) .$$

The solutions of this are

$$\bar{\chi} \propto e^{\pm i k_0 \vartheta}/\vartheta . \tag{77}$$

If k_0 is purely real, $\bar{\chi}$ decays as $\vartheta \to \infty$ for either sign. Thus, as in the MHD ballooning continuum, Eq. (74) has a continuum of formal solutions. Now, however, $k_0 \in \mathbb{R}$ corresponds to ω with $\mathrm{Im}(\omega) > 0$, when $\eta > 0$.

This can be most easily seen analytically by considering the case $\omega >> \omega_s$, similar to part C. We take $T_e/T_i = 0$. Then

$$k_0^2 = \frac{\omega[\omega - \omega_*(1+\eta)]}{\omega_A^2} - 7C\Big\{ \sum_{n\neq 0} |a_n|^2 \Big[1 - \frac{\omega_{*n}(1+2\eta)}{\omega}\Big]$$

$$- i\sqrt{\pi} \sum_{n\neq 0} |a_n|^2 \Big[\Big(1 - \frac{\omega_{*n}}{\omega}\Big)\Omega_n^5 - \eta \frac{\omega_{*n}}{\omega} \Omega_n^7\Big] e^{-\Omega_n^2}\Big\}$$

$$C = \frac{P}{q'^2} \Big\langle \frac{B^2}{|\nabla\psi|^2} \Big\rangle . \tag{78}$$

First, neglect the Landau damping term. Then this can be written as a cubic equation with real coefficients; unless all three roots are real, one has $\mathrm{Im}(\omega) > 0$. The criterion for instability can be obtained by standard procedures for cubic equations,

$$\frac{1+2\eta}{1+\eta} > \frac{1}{C'} \Big[\frac{C''}{3} + \frac{2}{27} + 2\Big(\frac{C''}{3} + \frac{1}{9}\Big)^{3/2}\Big] \tag{79}$$

where

$$C' = 7\omega_A^2 C \sum_{n\neq 0} |a_n|^2/(1+\eta)^2\omega_*^2$$

$$C'' = C' + k_0^2\omega_A^2/(1+\eta)^2\omega_*^2 .$$

The minimum value of the right-hand side of Eq. (79) is 1, and is attained when $C'=1$ and $k_0 = 0$. Thus $\eta>0$ is necessary for instability. Instabilities arise for $C''\sim 1$ and $\eta\sim 1$. This corresponds to $\omega_* \sim \varepsilon^{1/2}\omega_A$. As in the previous section, parallel dynamics should generally be included for this case, except if $q >> 1$.

If k_0 increases sufficiently so that all roots of the cubic equation are real, then the Landau resonance term still gives an instability with ω near the largest root of the cubic. The Landau term eventually becomes exponentially small for large k_0 or large ω_*; however, because of the large polynomial weighting, this requires $\Omega \gtrsim 3-4$.

As k_0 increases further, another mode branch becomes unstable for sufficiently large η. This is related to electrostatic η_i driven modes,[18] and arises because the denominator of the second term in $G_k^T(\Omega)$ can vanish. Assuming a particular $|a_n|$ is dominant, we can rewrite Eqs. (75)-(76)

$$1 + \frac{T_i}{T_e} + \Omega\ [(1 - \frac{\omega_{*n}}{\omega}Z(\Omega) - \eta\ \frac{\omega_{*n}}{\omega}Z^T(\Omega)] =$$

$$\Omega^2[(1 - \frac{\omega_{*n}}{\omega})Z_1(\Omega) - \eta\ \frac{\omega_{*n}}{\omega}\ Z_1^T(\Omega)]^2/ \tag{80}$$

$$\{\frac{\omega[\omega-\omega_{*n}(1+\eta))]}{\omega_A^2} - k_0^2)\frac{q'^2}{2p|a_n|^2}\left<\frac{B^2}{|\nabla\psi|^2}\right>^{-1} + \Omega\{(1 - \frac{\omega_{*n}}{\omega})Z_2(\Omega) - \eta\ \frac{\omega_{*n}}{\omega}\ Z_2^2(\Omega)\}.$$

The left side above is the local dispersion relation for collisionless electrostatic η_i modes for small $k_\perp \rho_i$ and adiabatic electrons.[18] For $\omega \sim \omega_{*i}$ and $k_0 \sim 1$, the right-hand side is $\sim \beta$. Thus for $\beta << 1$, the mode frequence is only slightly perturbed from the electrostatic case. Note, however, that these are toroidally induced modes, since Eq. (74) requires geodesic curvature. They are unstable for $\eta_i > 2$.[18] This η_i threshold is substantially higher than for the previous mode, unless β is much less than β_c.

The spectrum of Eq. (75) for the Connor model is shown in Fig. (7), for $T_e = T_i$, $\eta = 1$. There are several roots, one of which has $\mathrm{Im}(\omega) > 0$.

At sufficiently high ϑ, Eq. (74) breaks down, due to FLR effects ($\nabla s \rho_i \sim 1$), electron dissipation, etc. For example, $\nabla s \rho_i \sim 1$ when $\vartheta \sim 1/\varepsilon \hat{s}$. For realistic parameters, it is only possible to fit in at most 1 or 2 wavelengths (given by $2\pi/k_0$) in this range without k_0 becoming large enough to result in stability. The effects at high ϑ quantize the continuum; thus, Eq. (25) should be looked upon as only one component of an analysis to examine unstable eigenmodes. However, in the limit $\varepsilon \hat{s} \to 0$, instabilities are essentially guaranteed for $\omega_* \sim \varepsilon^{1/2} \omega_A$, for γ much less than β_c.

Physically, the salient point is that a wave packet exponentially grows as it propagates according to Eq. (74)-(75). The group velocity is typically small (and vanishes as $k_0 \to 0$), so several exponentiations are possible before reaching large ϑ.

E. Aspects of the Problem of Eigenmodes with Temperature Gradients

If we demand exponentially decaying eigenmodes, and apply the analysis used in Sec. VIIB including temperature gradients, we obtain

$$\frac{-\delta\Delta W \bar{J}^2 \left\langle \frac{B^2}{|\nabla\psi|^2} \right\rangle}{\chi_\infty^2 q'^2 A(\nu)} = (-k_0^2)^\nu \ . \tag{81}$$

When the plasma is slightly MHD unstable, this gives a decaying eigenmode with frequency close to the solution of $k_0 = 0$; ;this corresponds to the tip of the continuum in Fig. 1. An important point is that as $\delta\Delta W \to 0$ from negative values, the resulting instability has a non-vanishing growth rate, given by $k_0 = 0$. A graph of this growth rate vs. ω_* is shown in Fig. 8 for representative parameters.

The question then immediately arises as to the existence of unstable eigenmodes for $\delta\Delta W > 0$. These in fact are not allowed by Eq. (81); the proper branch cut of the fractional power ν corresponds to having the real part of the right-hand side always greater than or equal to zero, if we demand that the eigenfunction must exponentially decay.

Applying outgoing wave boundary conditions would also fail to give an eigenmode; the right-hand side would then have an imaginary part which could not be balanced by $\delta\Delta W$.

Eigenmodes for $\delta\Delta W < 0$ are only possible if additional effects are included.

1) The contribution to k(f) from the regions of the k integral other than $k = \pm 1, \pm 2, \ldots,$ these were neglected in Eq. (81) and in Sec. VIIC.

2) Physical effects at high ϑ, $\nabla s \rho_i \sim 1$, can be included, leading to a different boundary condition than that implied by Eq. (81).

The first type of terms would correspond to putting more driving energy in at $\vartheta \sim 1$, due to an FLR modification of the pressure response at $\vartheta \sim 1$. The second type of term would correspond to damping or partial reflection at high ϑ, thereby allowing the energy input mechanisms of the last section to result in a rigorous mathematical eigenmode.

Analytic results for either case are quite arduous to obtain, and will not be attempted here. Numerical analysis by Hastie and Hasketh,[5] Cheng,[6] Dominguez and Moore[9] and Teng[8] have found such instabilities.

VII. Conclusions

We have derived the dispersion relation for MHD modes with compressibility near marginal stability, Eq. (50). The net pressure expansion energy is absorbed primarily by compression and sonic energy production. We have given a kinetic formulation, for small aspect ratio, and Maxwellian equilibria. There are many formal similarities between the modified MHD variational principle, Eq. (16) and (19), and the kinetic analogues: the fluid propagator is replaced by a kinetic version, Eq. (61), (71), and (76). When finite larmor radius effects are neglected, the growth rates of the modes can be shown to always be less than the MHD case (though the marginal stability point is of course the same). Very near β_c, the growth rates are much less, and scale differently, Eq. (64), due to ion parallel Landau resonances.

Because of the reduced growth rate, ω_* effects become important for low mode number in both fluid and kinetic cases.

When only density gradients are considered, ω_* was often found to increase the growth rates when $\omega_* \lesssim \varepsilon^{1/2}\omega_A$, but the marginal stability point was unchanged. For the fluid ion case, the dispersion relation, when $\omega_* << \omega_s$, Eq. (69), revealed that the cause of instability was a resonance in the fluid sound wave propagator. For $\omega_* >> \omega_s$, Eq. (73), the FLR effects change the sign of the perpendicular compressibility contribution so that it becomes destabilizing rather than stabilizing. With collisionless ions (and small shear or very small aspect ratio), Eq. (71), there is always instability when $\Delta W<0$ due to parallel Landau resonances. The growth rates, Fig. (5)-(6), are often increased over the ideal MHD values.

With temperature gradients and collisionless ions, a new source of energy is introduced at large ϑ, independent of the MHD drive. Modes corresponding to the continuum, Eqs. (74)-(77), are now unstable, Because of this, at $\beta=\beta_c$, the growth rate is finite, rather than zero, Eq. (81). The magnitude of the kinetic growth rate at $\beta = \beta_c$ corresponds to the value which would arise in the full MHD case for β exceeding β_c by 20-30%. These instabilities are most intense for $\omega_* \sim \varepsilon^{1/2}\omega_A$. The existence of unstable eigenmodes for $\beta < \beta_c$ depends on the degree of damping arising at high ϑ due to dissipative effects not considered here.

The kinetic analysis reveals that as $\beta \to \beta_c$, instabilities first arise with mode number n corresponding to $\omega_* \sim \varepsilon^{1/2}\omega_A \sim \omega_s$. Such effects may therefore determine whether kink modes or ballooning modes limit β.

Appendix A: Equivalence of Matching to the Procedure of Section III

We show the equivalence between the variational technique and matching.

Define projection operators to separate out the slowly varying and rapidly varying parts of a given $\Phi(\vartheta)$, by

$$\bar{P}\Phi = \int_{-K_0}^{+K_0} \frac{dk}{2\pi}\, ik\vartheta \int_{-\infty}^{+\infty} d\vartheta\ \Phi(\vartheta) e^{ik\vartheta} \tag{A.1}$$

and $\tilde{P} = 1-\bar{P}$. We take $(\gamma/\omega_s) \to 0$, and choose $\gamma/\omega_s << K_0 << 1$. Then

$$\frac{\partial^2 \tilde{f}}{\partial\vartheta^2} = \frac{2\Gamma\bar{p}}{\bar{J}} \frac{\gamma^2}{\omega_s^2} \tilde{P}(J\kappa_\omega \chi) \tag{A.2}$$

and

$$\frac{\partial^2}{\partial\vartheta^2} \bar{f} + \frac{\gamma^2}{\omega_s^2} \bar{f} = \frac{2\Gamma\bar{p}}{\bar{J}} \frac{\gamma^2}{\omega_s^2} \tilde{P}(J\kappa_\omega \chi) \ . \tag{A.3}$$

For $\vartheta > \vartheta_c$, take χ_T to be the solution of

$$\frac{\gamma^2 |\nabla S|^2}{B^2} \rho\chi_T + 2\kappa_\omega \tilde{f}_T - \frac{\partial}{\partial\vartheta} \frac{|\nabla S|_c^2}{JB} \frac{\partial}{\partial\vartheta} \chi_T + \kappa_{\omega_c} \chi_T = 0 \ . \tag{A.4}$$

For $\vartheta < \vartheta_c$, $\chi_T = \chi_c$. This is essentially equivalent to Eq. (32). Note that $\partial\chi_T/\partial\vartheta$ is not continuous at $\vartheta=\vartheta_c$.

The difference $\delta\chi_T$ between χ and χ_T satisfies

$$\gamma^2 \frac{|\nabla s|^2}{B^2} \rho \ \delta\chi_T + 2\kappa_\omega \delta\tilde{f}_T - \frac{\partial}{\partial\vartheta} \frac{|\nabla S|^2}{JB} \frac{\partial}{\partial\vartheta} \delta\chi_T + 2\kappa_\omega \delta\chi_T$$

$$- (\gamma^2 \frac{\nabla S^2}{B^2} \rho \ \chi_T + 2\kappa_\omega \tilde{f}_T - \frac{\partial}{\partial\vartheta}$$

$$\frac{|\nabla S|^2}{JB} \frac{\partial}{\partial\vartheta} \chi_T + 2\delta\kappa_\omega \chi_T) + [\gamma^2 \frac{\delta|\nabla S|^2}{B^2} \rho - \frac{\partial}{\partial\vartheta} \frac{\delta|\nabla S|^2}{JB}$$

$$\frac{\partial}{\partial\vartheta} + 2\delta\kappa_\omega](\chi_T + \partial\chi_T) + 2\kappa_\omega(\bar{f}_T + \delta\bar{f}_T) = 0 \qquad \text{(A.5)}$$

where $\frac{\partial}{\partial\vartheta^2} (\bar{f}_T + \delta\bar{f}_T) + \frac{\gamma^2}{\omega_s^2} (\bar{f}_T + \delta\bar{f}_T) = \frac{2\Gamma_{\bar{p}}}{\bar{J}} \bar{P}[J\kappa_\omega(\chi_T + \delta\chi_T))]$.

We now compute $\delta\chi$ to lowest order in δ, i.e., we neglect $\delta\chi$ and $\delta\bar{f}$ relative to χ_T and f_T. To obtain $\delta\chi(\vartheta)$, multiply Eq. (A5) by χ_T and integrate from 0 to slightly below ϑ_c, and from slightly above ϑ_c to ∞. Integrating by parts,

$$\frac{|\nabla S|^2}{J^2 B} c(\chi_c \frac{\partial}{\partial\vartheta} \chi_c + \chi_c \frac{\partial\delta\chi}{\partial\vartheta} - \delta\chi \frac{\partial\chi_c}{\partial\vartheta})$$

$$= \frac{1}{\bar{J}} \int_0^{\vartheta_c} d\vartheta J \ \gamma^2 |\nabla S|^2 \chi_T^2 + \frac{|\nabla S|^2}{J^2 B^2} (\frac{\partial\chi_T}{\partial\vartheta})^2 + 2\chi_\omega p' \chi_T^2 \qquad \text{(A.6)}$$

$$+ \frac{1}{\bar{J}} \int_0^{\vartheta_c} d\vartheta \ 2J\kappa_\omega \chi_T (\bar{f} + \tilde{f})$$

and

$$- \frac{|\nabla S|^2}{J^2 B^2} \left(\chi_T \frac{\partial}{\partial\vartheta} \chi_T + \chi_T \frac{\partial \delta\chi_T}{\partial\vartheta} - \delta\chi_T \frac{\delta\chi_T}{\partial\vartheta}\right) \tag{A.7}$$

$$= \frac{1}{J} \int_{\vartheta_c}^{\infty} d\vartheta \; \gamma^2 |\nabla S|^2 \chi_T^2 + \frac{|\nabla S|^2}{J^2 B^2} \left(\frac{\partial\chi_T}{\partial\vartheta}\right)^2 + 2\kappa_\omega \rho' \chi_T^2$$

$$+ \frac{1}{J} \int_{\vartheta_c}^{\infty} d\vartheta \; 2J\kappa_\omega \chi_T (\bar{f} + \tilde{f}) \; .$$

$\chi_T + \delta\chi$ should have a continuous logarithmic derivative across ϑ_c. Note that to first order

$$\chi_T^2 \left[\frac{\partial}{\partial\vartheta} (\chi_T + \delta\chi)\right] / (\chi_T + \delta\chi) = \chi_T \frac{\partial}{\partial\vartheta} \chi_T + \chi_T \frac{\partial\delta\chi_T}{\partial\vartheta} - \delta\chi_T \frac{\partial\chi_T}{\partial\vartheta} \; .$$

Since χ_T is continuous, we require the right-hand side of Eq. (A.6) to be continuous with Eq. (A.7); this gives the dispersion relation, Eq. (16), $V(\chi_T) = 0$. We thus see that the variational formulation is equivalent to matching the interior region solution, $\chi_T + \delta\chi$ to the exterior region solution, $\chi_T + \delta\chi$ where $\delta\chi$ gives the effects of $\bar{f}$ on $\bar{\chi}$ as a perturbation. The fact that the dispersion relation is independent of ϑ_c (to lowest order) means that there exists an intermediate region in ϑ in which the form of $\chi_c + \delta\chi$ and $\chi_T + \delta\chi$ are the same, so that this is an asymptotic matching procedure. This similarity in form can also be justified a posteriori.

Appendix B: Intermediate Results of Two-Scale Analysis

To obtain Eq.(21)-(22), note that for large ϑ and small γ,

$$q'^2\left[\left\langle\frac{|\nabla\psi|^2}{JB}\right\rangle_M \frac{\partial}{\partial\vartheta}\vartheta^2\frac{\partial}{\partial\vartheta}\bar{\chi}+\frac{\partial}{\partial\vartheta}\vartheta^2\left\langle\frac{|\nabla\psi|^2}{JB}\frac{\partial\tilde{\chi}}{\partial\vartheta}\right\rangle_M\right]$$

$$+\ 2\langle J\kappa_\omega\rangle(p'\bar{\chi}+\bar{f})\ +\ 2\langle J\kappa_\omega(p'\tilde{\chi}+\tilde{f})\rangle=\gamma^2\ \rho\ q'^2\langle J|\nabla\psi|^2/B^2\rangle_M\vartheta^2\bar{\chi},$$

$$\frac{\partial\tilde{\chi}}{\partial\vartheta}=-\left(1-\frac{JB^2/|\nabla\psi|^2}{\langle JB^2/|\nabla\psi|^2\rangle_M}\right)\frac{\partial\bar{\chi}}{\partial\vartheta}$$

$$-\ \frac{(\bar{\chi}+\bar{f}/p')}{\vartheta q'}\left(\frac{\sigma JB^2}{|\nabla\psi|^2}-\frac{\langle\sigma JB^2/|\nabla\psi|^2\rangle_M}{\langle JB^2/|\nabla\psi|^2\rangle_M}\right),$$

$$\frac{\partial\tilde{f}}{\partial\vartheta}=2\gamma^2p'\vartheta\left(JB^2\sigma-\langle JB^2\sigma\rangle_M/\langle JB^2\rangle_M\right),$$

and

$$2J\ \kappa_\omega\rightarrow\frac{\vartheta q'}{p'}\frac{\partial\sigma}{\partial\vartheta}.$$

We also use

$$\langle 2J\kappa_\omega\ \tilde{\chi}\rangle_M\rightarrow-\ \frac{\chi q'}{P'}\left\langle\sigma\ \frac{\partial\tilde{\chi}}{\partial\vartheta}\right\rangle_M,$$

$$\langle 2J\kappa_\omega\ \tilde{f}\rangle_M\rightarrow\frac{-\vartheta q'}{p'}\left\langle\omega\ \frac{\partial\tilde{f}}{\partial\vartheta}\right\rangle_M,$$

and $$\langle 2J\kappa_\omega\rangle_M=\langle 2J[\hat{b}\cdot\nabla\hat{b}\times B\cdot(q\nabla\vartheta-\nabla\zeta)]/B^2\rangle.$$

References

1. F. Troyon, F. Gruber, H. Saurenmann, S. Semenzato, and S. Succi, Plasma Physics and Controlled Fusion 25, (1984) 209.
2. W.M. Tang, J.W. Connor and R.J. Hastie, Nucl. Fusion 20, 1439 (1980).
3. K.T. Tsang, Phys. Fluids 24, 2017 (1981).
4. H.R. Strauss, Phys. Fluids 26, 2219 (1983).
5. R.J. Hastie and K.W. Hasketh, Nucl. Fusion 21, 651 (1981).
6. C.Z. Cheng, Phys. Fluids 25, 1020 (1982).
7. C.E. Seyler and J.P. Freidberg, Phys. Fluids 23, 331 (1980).
8. W.M. Tang, G. Rewoldt, C.Z. Chang, and M.S. Chance, Nucl. Fusion 25, 151 (1985).
9. R.R. Dominguez and R.W. Moore, submitted to Nuclear Fusion.
10. H.R. Strauss, Phys. Fluids 20, 1354 (1977).
11. T.M. Antonsen, Jr., submitted to Nuclear Fusion.and B. Lane 23, 1205 (1980).
12. M.S. Chance, et al., Plasma Physics and Controlled Nuclear Fusion Research (Proc. 7th Int. Conf. Innsbruck, 1978) Vol. 1, IAEA, Vienna (1979) ~~799~~. 677
13. J.W. Connor, R.J. Hastie and J.B. Taylor, Phys. Rev. Lett. 40, 396 (1978).
14. T.M. Antonsen, Jr., A. Ferreira and J.J. Ramos, Plasma Physics 24, 197 (1982).
15. J.W. Van Dam, Ph.D. Thesis, University of California, Los Angeles, 1979.
16. A.H. Glasser, J.M. Green and J.C. Johnson,. Phys. Fluids 18, 875 (1975).
17. H.L. Berk, Plasma Physics and Controlled Nuclear Fusion Research (Proc. 10th Int. Conf. London, 1984, Vol. 2, IAEA, Vienna (1985) 321.
18. B.B. Kadomtsev and O.P. Pogutse, in Reviews of Plasma Physics, edited by M.A. Leontovich (Consultants Bureau, New York, 1970), vol. 5, p. 303.

Figure Captions

Fig. 1 – The stability boundaries $\beta_c(-)$ and $\beta_c'(---)$ for ballooning modes for small $\varepsilon(\varepsilon=.07)$. $\hat{s}$ is the shear parameter, and α is the poloidal β multiplied by ε.

Fig. 2 – Growth rates past β_c for $\hat{s}=.7$ and $\varepsilon=.07$ and $D_I=0$. The solid line is the full MHD case. Also shown are the analytic result, and the result when all compressibility effects are neglected.

Fig. 3 – Growth rates past β_c for $\hat{s}=.7$, $\varepsilon=.07$ and $D_I=-.3$. The solid line is the full MHD case. Also shown are the analytic result, and the result when all compressibility effects are neglected.

Fig. 4 – Fluid results for growth rates and real frequencies as ω_* is increased for $\alpha_c/\alpha = 1.04$, $\hat{s}=.7$ and $\varepsilon=.07$. The value $\omega_* = 2\gamma_{MHD}$ is noted.

Fig. 5 – Kinetic results for growth rates and real frequencies as ω_* is increased for $\gamma_{MHD}/\varepsilon^{1/2}\omega_A = .1$.

Fig. 6 – Kinetic results for growth rates and real frequencies as ω_* is increased for $\gamma_{MHD}/\varepsilon^{1/2}\omega_A = .5$.

Fig. 7 – The spectrum of the continuum (i.e., the solution of Eq. (75) for $k_0 \in \mathbb{R}$), for $\alpha=.3$, $\omega_{*n}=.3$, $T_e/T_i = 1$ and $\eta=1$. All frequencies are normalized to $\sqrt{\varepsilon}\ \omega_A$.

Fig. 8 – Kinetic results with temperature gradients for the growth rate and frequency at $\beta=\beta_c$ versus ω_*. For $\alpha=.46$, $T_e/T_i = 1$, $\eta=1$. All frequencies are in units of $\sqrt{\varepsilon}\ \omega_A$.

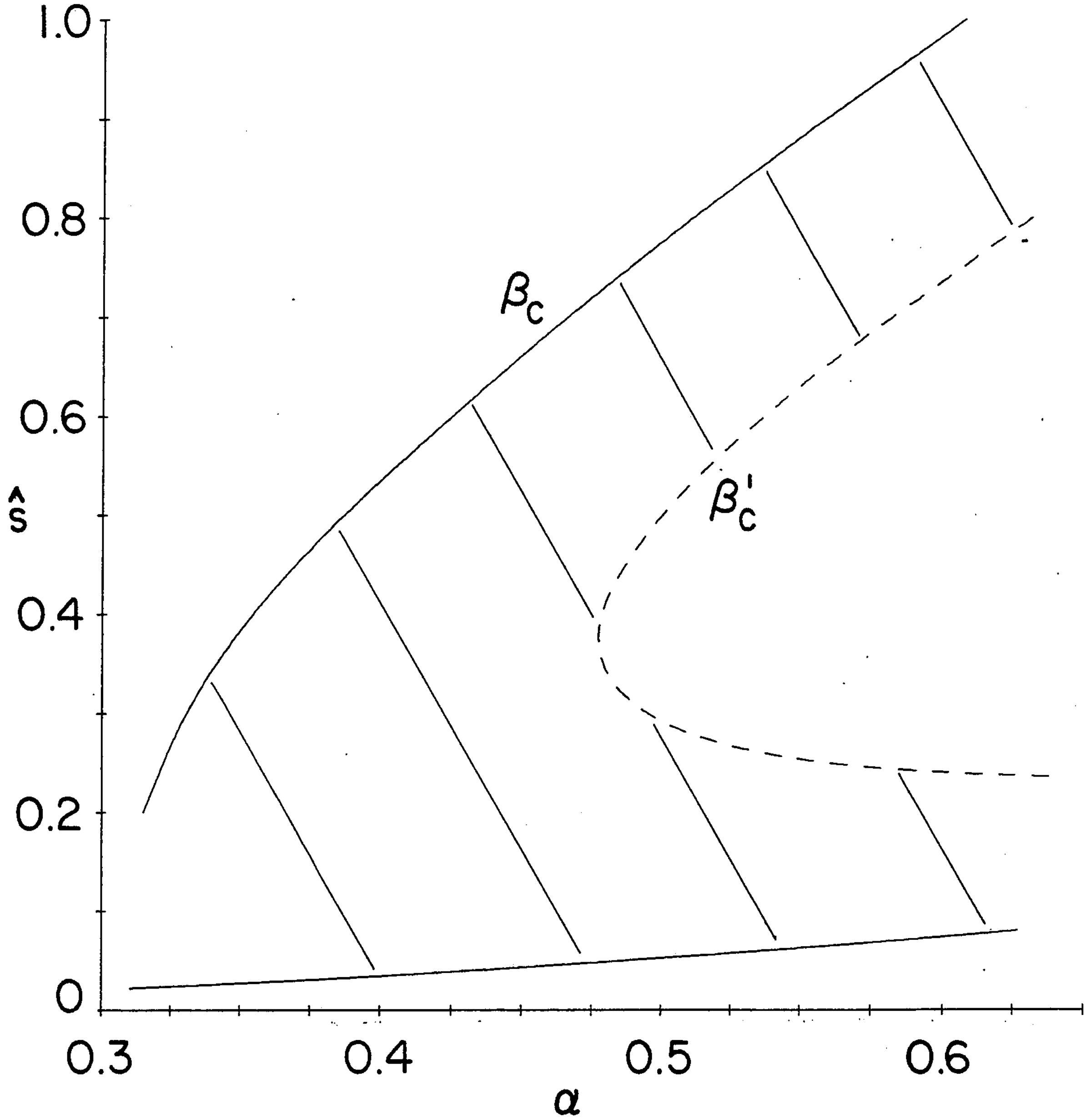

Fig. 1

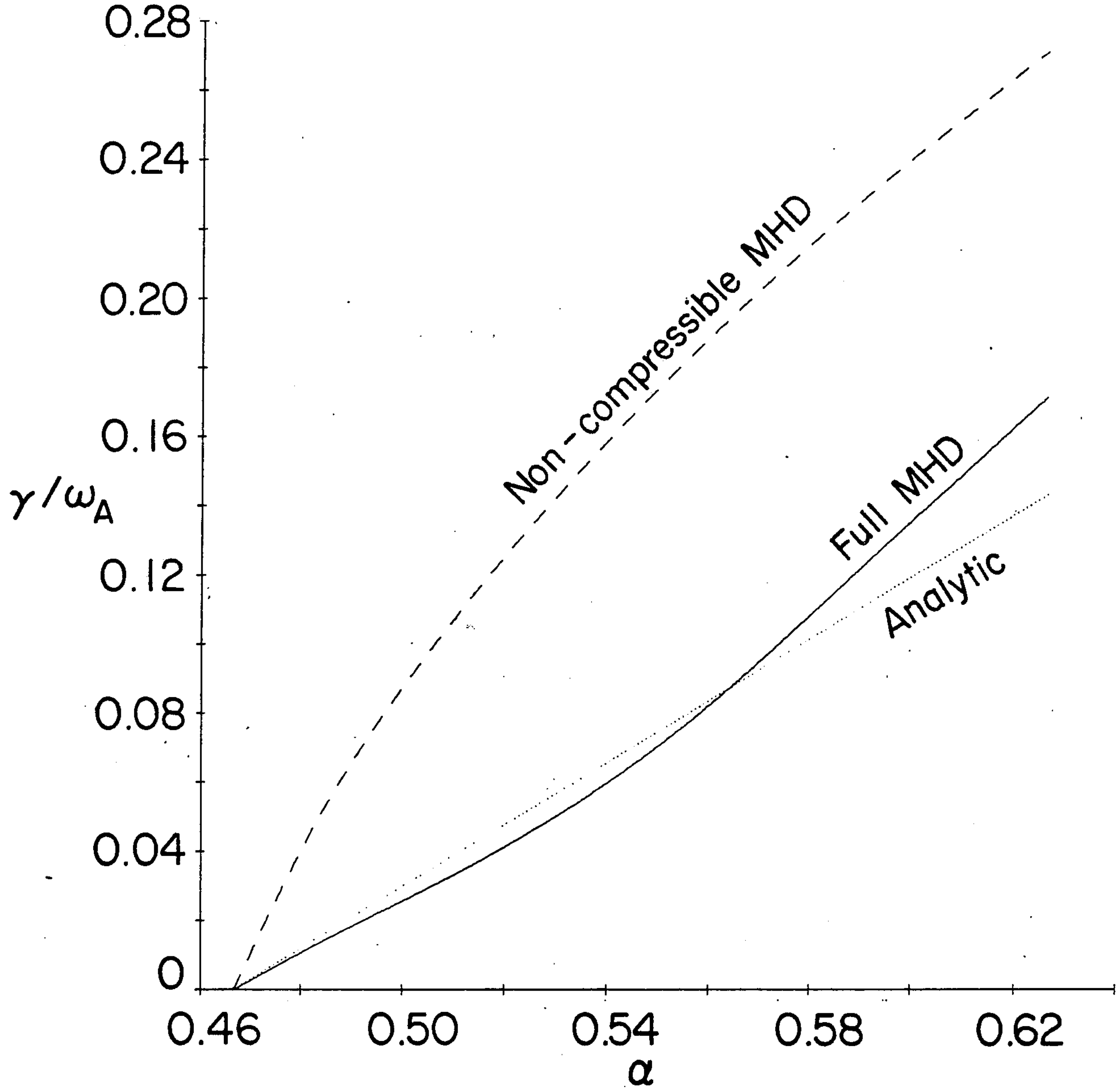
0.28
0.24
0.20
0.16
0.12
0.08
0.04
0
γ/ω_A
0.46
0.50
0.54
0.58
0.62
α
Non-compressible MHD
Full MHD
Analytic

Fig. 2

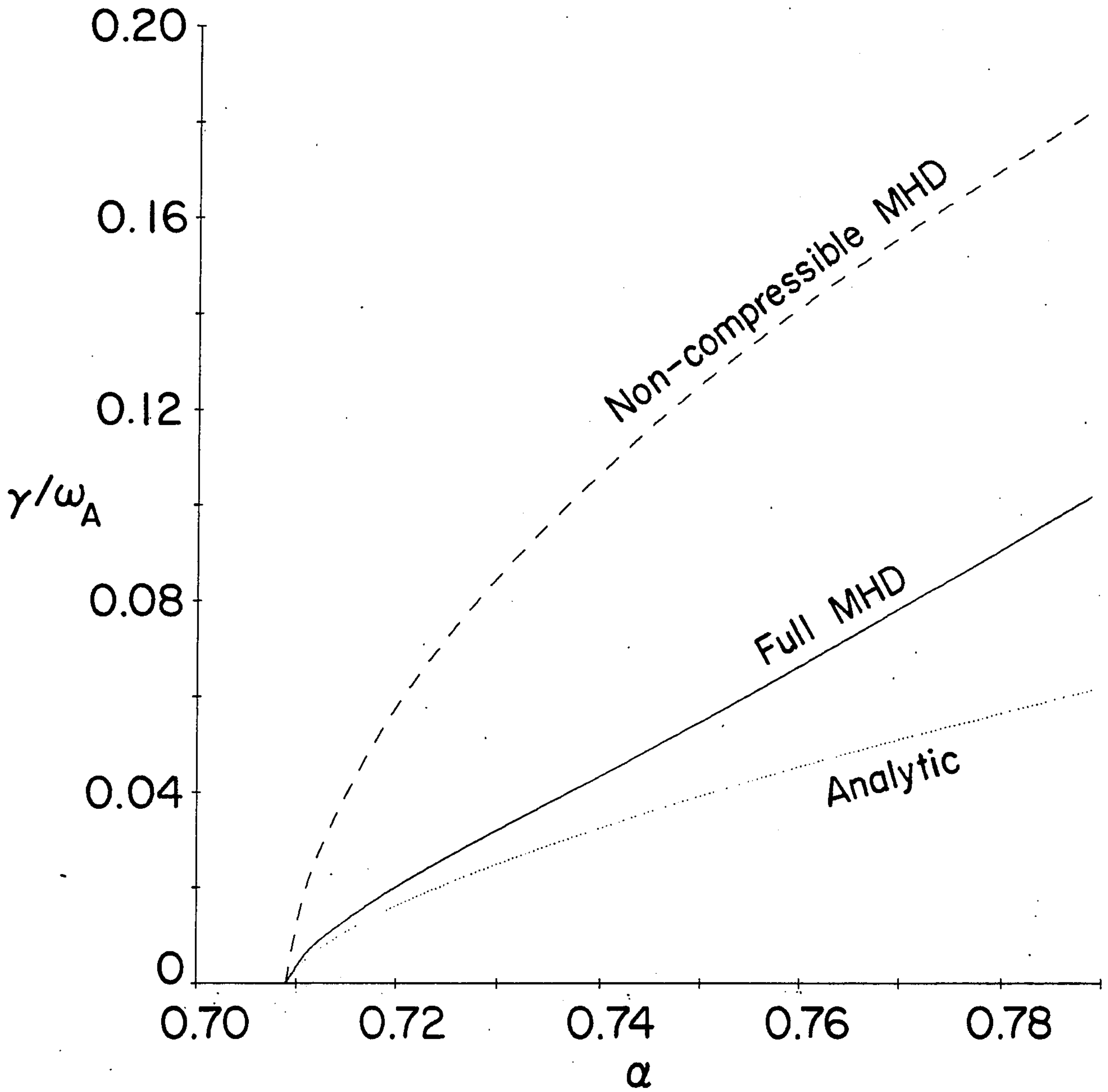

0.20
0.16
0.12
0.08
0.04
0
γ/ω_A
0.70
0.72
0.74
0.76
0.78
α
Non-compressible MHD
Full MHD
Analytic

Fig. 3

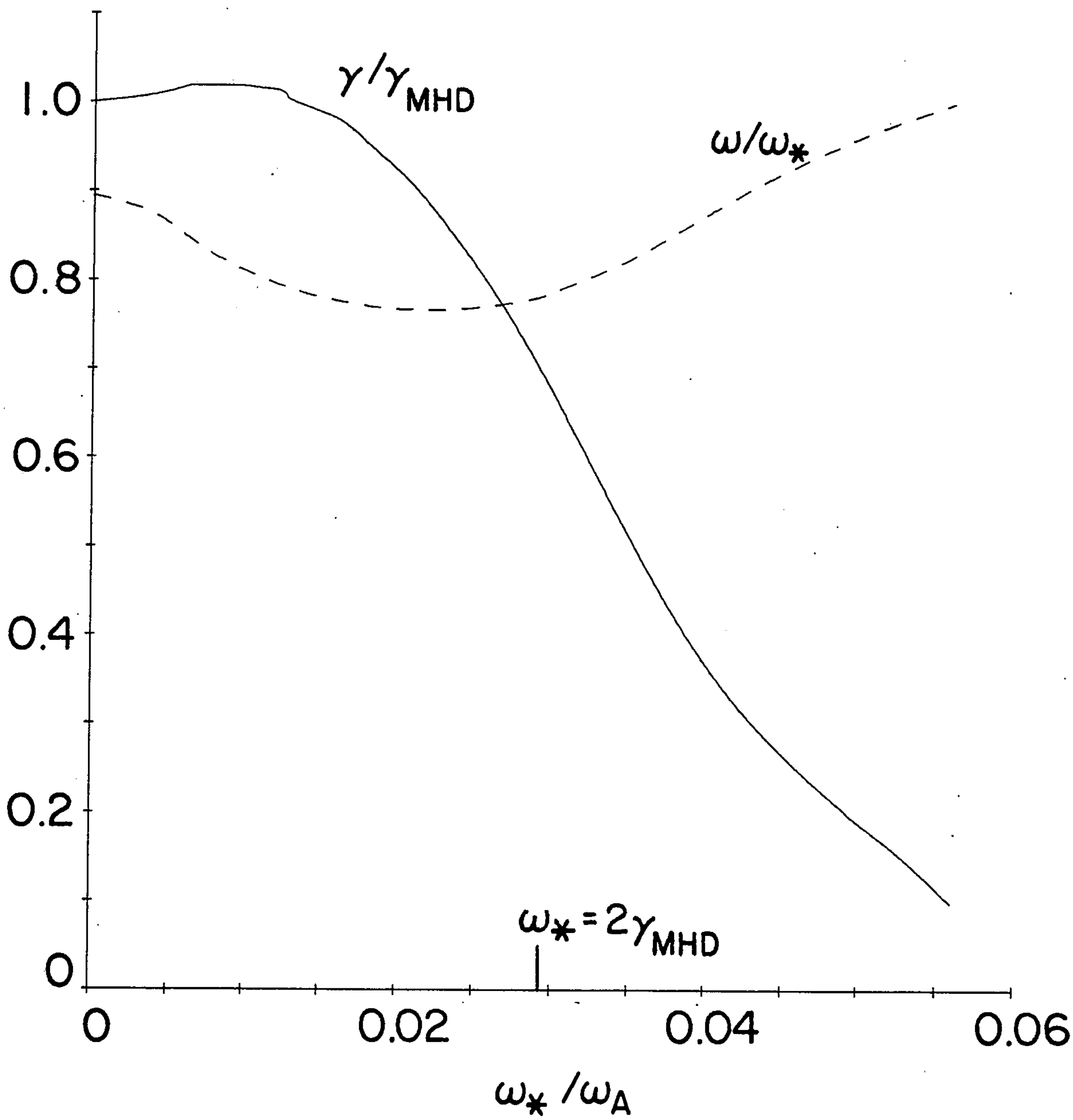

1.0
0.8
0.6
0.4
0.2
0
γ/γ_{MHD}
ω/ω_*
$\omega_* = 2\gamma_{MHD}$
0
0.02
0.04
0.06
ω_* / ω_A

Fig. 4

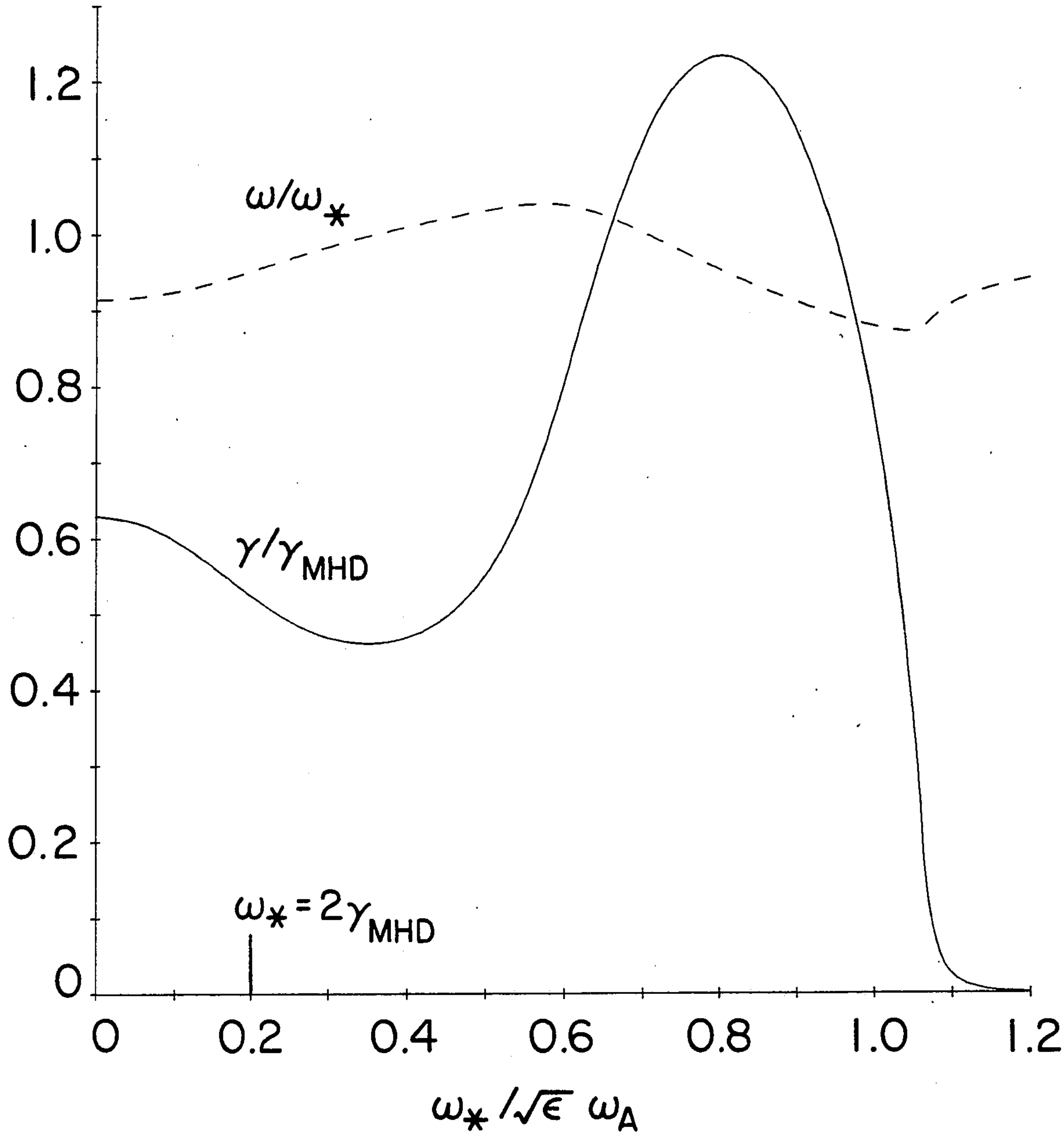

Fig. 5

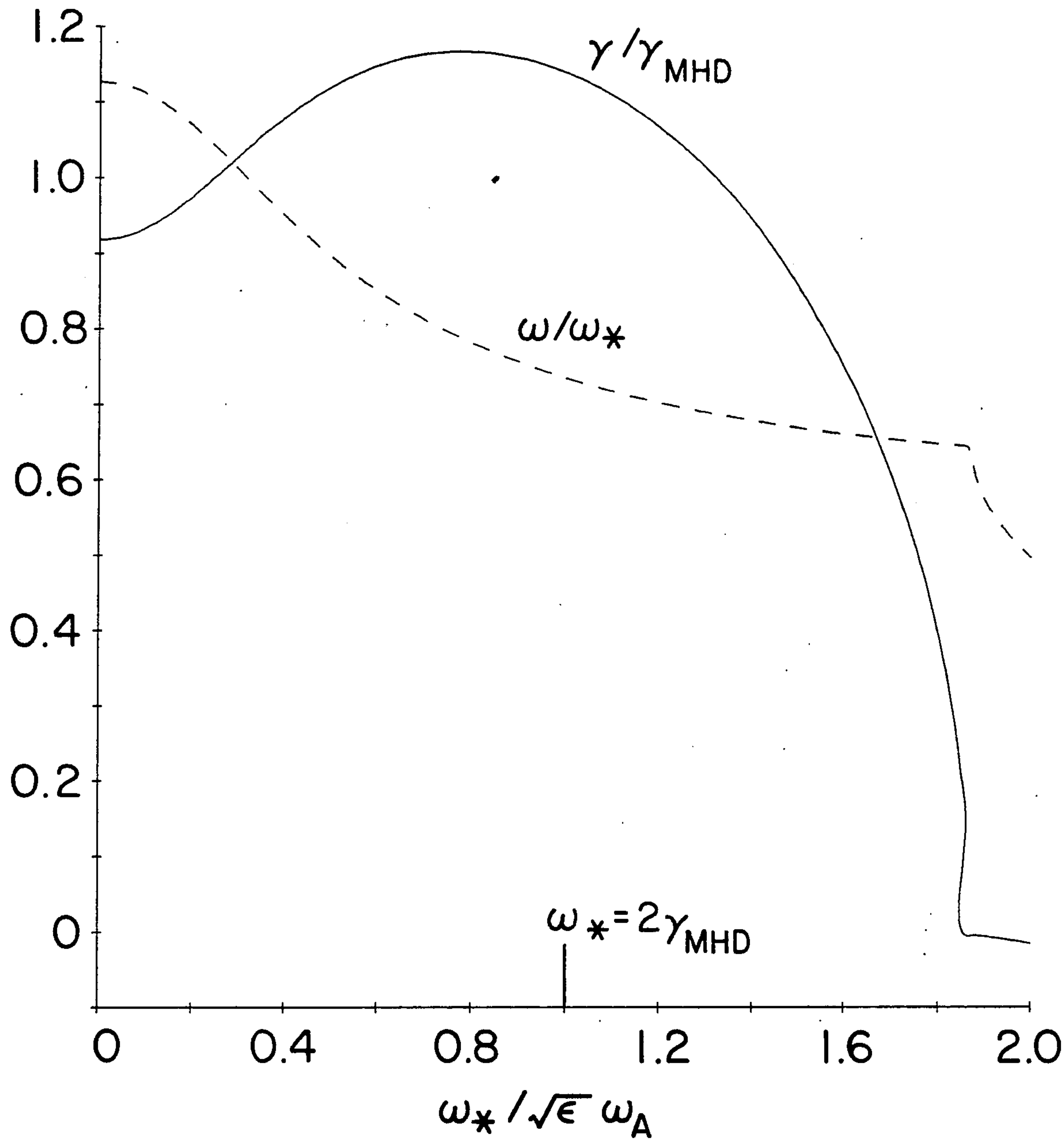

1.2
1.0
0.8
0.6
0.4
0.2
0
γ/γ_{MHD}
ω/ω_*
$\omega_* = 2\gamma_{MHD}$
0
0.4
0.8
1.2
1.6
2.0
$\omega_* / \sqrt{\epsilon}\, \omega_A$

Fig. 6

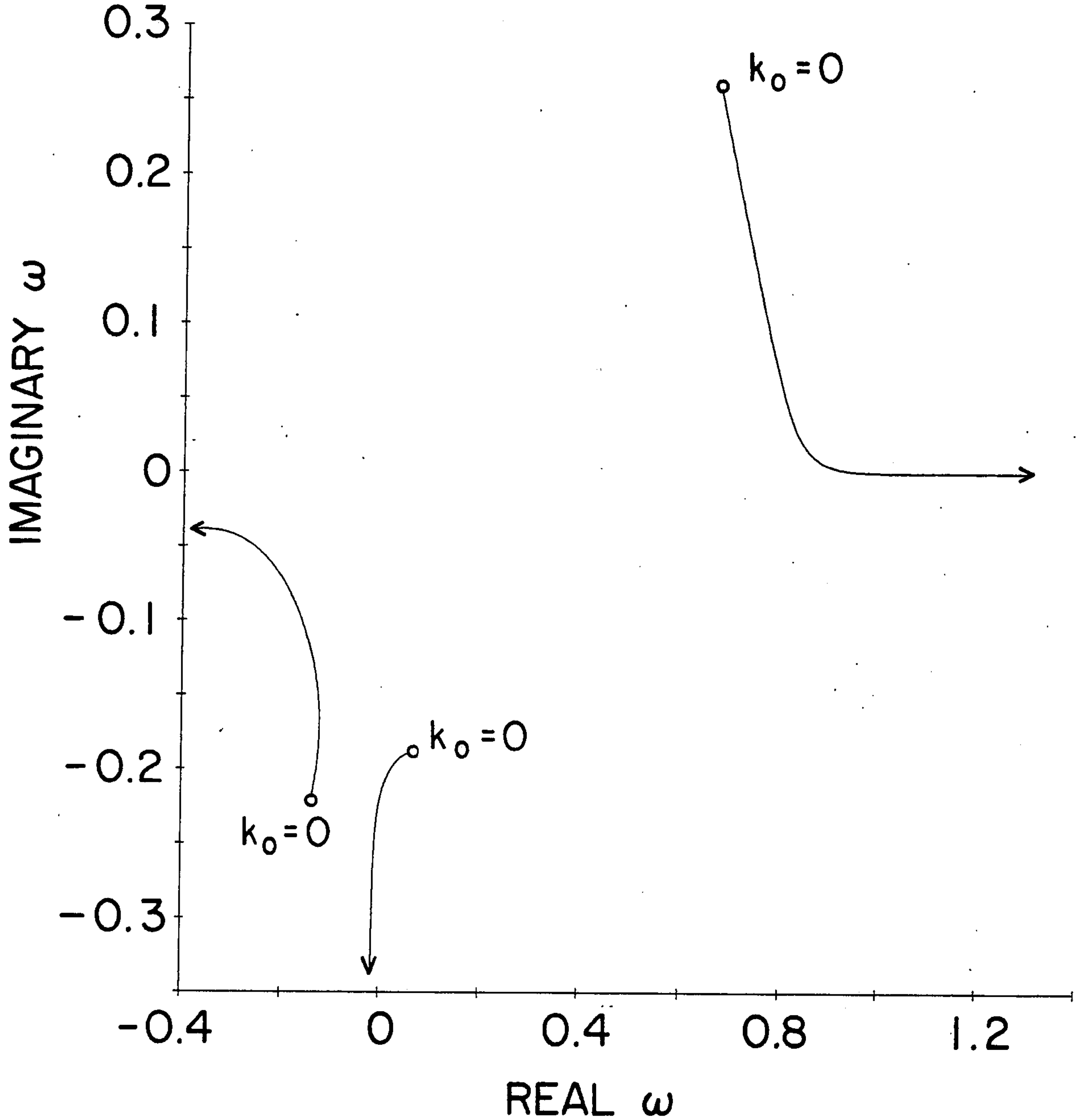

Fig. 7

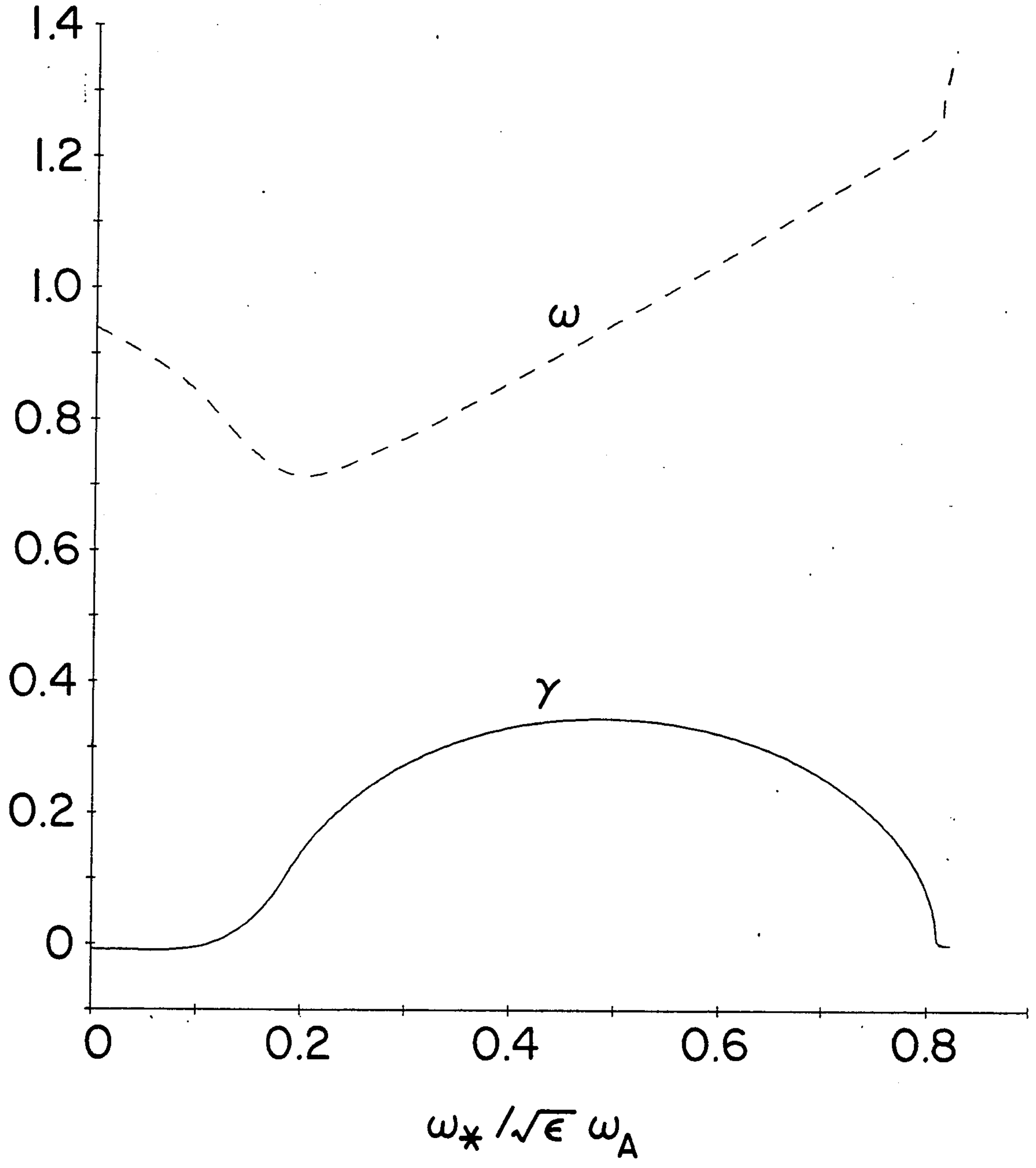

Fig. 8